

---

*Review***Synthesis routes of zeolitic imidazolate framework-8 for CO<sub>2</sub> capture:****A review****Angaraj Singh<sup>1</sup>, Ajitanshu Vedrtam<sup>1,2,\*</sup>, Kishor Kalauni<sup>1</sup>, Aman Singh<sup>3</sup> and Magdalena Wdowin<sup>2</sup>**<sup>1</sup> Department of Mechanical Engineering, Invertis University, Bareilly, UP, India-243001<sup>2</sup> Mineral and Energy Economy Research Institute, Polish Academy of Sciences, Wybickiego 7A, Krakow, Poland<sup>3</sup> Department of Ceramic Engineering, Indian Institute of Technology Varanasi, UP, India- 221005**\* Correspondence:** Email: [ajitanshu.m@invertis.org](mailto:ajitanshu.m@invertis.org).

**Abstract:** Zeolitic imidazole framework-8 (ZIF-8) represents a notable subtype of metal-organic frameworks (MOFs), characterized by tetrahedral and zeolite-like structures interconnected through Imidazolate anions. ZIF-8's outstanding attributes, including its expansive intra-crystalline surface area and robust chemical and thermal stability, have positioned it as a promising contender for carbon dioxide (CO<sub>2</sub>) capture applications. The application of ZIF-8 in the membrane and composite fields involves utilizing ZIF-8 in the development and enhancement of membranes and composite materials for gas separation, catalysis, and sensing. This article serves as a comprehensive exploration of contemporary CO<sub>2</sub> capture technologies, elucidating their respective merits and demerits. Moreover, the review offers insights into the prevailing CO<sub>2</sub> adsorption techniques implemented across industries. Delving into ZIF-8 synthesis methods, the discourse encompasses diverse synthetic pathways. Experimental evidence, furnished through X-Ray diffraction patterns and scanning electron microscopy, validates ZIF-8's structure-activity correlation and morphological characteristics. We extend this review to encapsulate the parameters governing CO<sub>2</sub> adsorption by ZIF-8, delineating the key factors influencing its capture efficacy. Notably, we encompass CO<sub>2</sub> measurement protocols and techniques specific to ZIF-8. Additionally, we appraise the CO<sub>2</sub> adsorption potential of ZIF-8 within various composite and filter systems composed of distinct ZIFs. Culminating with an emphasis on ZIF-8's exceptional advantages for CO<sub>2</sub> capture, this review serves as a repository of insights into the unparalleled potential of ZIF-8 as a foundational material. Providing a succinct yet comprehensive

overview, this article facilitates a rapid understanding of ZIF-8's transformative role in the realm of CO<sub>2</sub> capture.

**Keywords:** CO<sub>2</sub> uptake; filter; metal-organic framework; synthesis route, zeolites; ZIF-8

## 1. Introduction

CO<sub>2</sub> is widely recognized as a greenhouse gas and the principal cause of global warming, which has been amplified by the usage of fossil fuels [1]. A report suggests that the level of CO<sub>2</sub> has increased by about 100 ppm compared to the last six decades and is predicted to increase further because of the continuous usage of fossil fuels as the primary energy source [2,3]. The reduction in CO<sub>2</sub> emission and adsorption/capturing of CO<sub>2</sub> are challenging issues around the globe as the CO<sub>2</sub> pollution may increase the greenhouse effects, climate changes, snow cover melts, etc. [4,5]. The advancement of CO<sub>2</sub> capture and separation systems is ongoing. Recently, membrane separation, physical adsorption, and chemical absorption have been used to adsorb/separation of CO<sub>2</sub>. Among the existing techniques, membrane separation (metal-organic framework) is one of the efficient techniques to adsorb/separate CO<sub>2</sub> due to its low energy consumption, easy industrialization, high economic benefits, and high efficiency [4,6]. The metal-organic framework (MOF) is porous crystalline compounds with metal ions linked by organic linkers [7]. MOFs are the fastest emerging fields in chemistry because of their structural and functional tunability. MOFs are used for CO<sub>2</sub> uptake/capture due to their high porous structure, thermal and chemical stability, and large surface area [8,9]. Among the MOFs, zeolitic imidazolate frameworks (ZIFs), a sub-family of MOFs, are popular due to their advanced features like high surface area, porous structure, and flexibility towards permeability. ZIFs are porous hybrid materials with zeolitic-like structures [10]. ZIFs are formed of a divalent metal cation (e.g., Zn<sup>2+</sup> or CO<sup>2+</sup>) connected to nitrogen atoms in an anionic imidazolate molecule, resulting in tetrahedral frameworks [11]. They are composed of a Zn<sup>2+</sup> metal cation that is linked with molecules of the organic linker 2-methylimidazole (2-mIm), resulting in huge cavities of 1.16 nm interconnected with windows of approximately 0.34 nm [12].

ZIF-8 has been widely used as a filter material for gas separation (CO<sub>2</sub>, H<sub>2</sub>, and CH<sub>4</sub>) due to its higher chemical and thermal stability and flexibility [13]. ZIF-8 is a potential gas storage material. It was claimed that the adsorption and desorption process for ZIF-8 was reversible with no hysteresis, indicating a rapid adsorption and desorption process. ZIF-8's porous nature and wide surface area make it an excellent material for gas storage applications [14]. Despite ZIF-8 being well-known for its flexibility, the presence of H<sub>2</sub> (kinetic diameter of 0.29 nm) is expected to be preferred over that of CO<sub>2</sub> (0.33 nm) [15]. ZIF-8 has shown excellent chemical resistance, remaining unchanged after seven days of immersion in boiling methanol, benzene, and water, as well as 24 h of immersion in concentrated sodium hydroxide at 100 °C [16].

ZIF-8 is simple to synthesize and exhibits a molecular sieving action, resulting in exceptional CO<sub>2</sub> selectivity and permeability [17]. It has been reported that in the separation of CO<sub>2</sub>/CH<sub>4</sub>, ZIF-8 demonstrates the highest permeability ( $240 \times 10^{-7} \text{ mol m}^{-2} \text{ s}^{-1} \text{ Pa}^{-1}$ ) and selectivity ( $\sim 7$ ) among all the reported ZIFs (ZIF-7, ZIF-67, ZIF-90, and ZIF-9-67) [18]. ZIFs are based on tetrahedral topologies and are created by connecting 4-coordinated transition metals by imidazolate with an angle of 145°.

The M-Im-M (M = Zn or CO and Im = imidazolate) angle is responsible for the synthesis of a large number of ZIFs with Zeolitic-type-tetrahedral topologies [19]. ZIF-8 is synthesized using different routes; however, the CO<sub>2</sub> uptake or capture by ZIF-8 depends on the chosen synthesis route [20]. Several factors come into play when approaching the synthesis process of ZIFs; some are geometry, maintenance, functionality, conformation, compatibility, solubility, pH, temperature, etc. [21,22]. The structure of ZIFs mainly depends on the category of imidazolate and solvents used. Moreover, the structural diversity in ZIFs is due to the use of functionalized imidazolate ligands in the synthesis process [23,24]. In view of the above, our objective of this review is to summarize the synthesis routes of ZIF-8 and their outcomes in terms of CO<sub>2</sub> adsorption. We also focus on factors affecting CO<sub>2</sub> capture/adsorption. The techniques used for CO<sub>2</sub> adsorption are also discussed briefly.

## 2. Current technologies for CO<sub>2</sub> capture

The capture/storage of CO<sub>2</sub> is a process in which CO<sub>2</sub> is captured from different sources such as industry, fossil fuels, and wastes before its interaction with the atmosphere. The emitted CO<sub>2</sub> is compressed and injected deep enough for everlasting storage [25,26]. Three CO<sub>2</sub> capturing techniques were developed: (i) the post-combustion capture process, (ii) the pre-combustion capture process, and (iii) the oxy-combustion process [27].

In the post-combustion capture process, CO<sub>2</sub> is produced in a regular way from burnt fuel, and then organic solvents are used to remove CO<sub>2</sub> from the air [28]. In the pre-combustion technique, oxygen and steam are used to convert fuel into hydrogen and CO<sub>2</sub> and then capture CO<sub>2</sub> with the help of solvents or solid absorbents [29]. In this process, CO<sub>2</sub> is captured before fuel is burned. Further, in the oxy-firing process, the fuel is burned in pure oxygen and converted into water vapor and CO<sub>2</sub>. After cooling the burning gas, the water vapor is condensed, and CO<sub>2</sub> is captured [30].

The most significant method of CO<sub>2</sub> removal is sorption, which includes independent adsorption and absorption [31]. In the literature, a number of CO<sub>2</sub> adsorbing/absorbing materials have been documented [32]. The adsorbent material used for absorption has (a) high selectivity; (b) high CO<sub>2</sub> adsorption capacity at high temperature; (c) good adsorption/desorption kinetics; (d) stable adsorption capacity after repeated cycles; and (e) adequate mechanical strength of adsorbent particles for cyclic exposure [33].

Furthermore, carbon-based adsorbents and metal oxide adsorbents such as CaO, MgO, hydrotalcite-like compounds (HTICs), and zeolites, are employed for CO<sub>2</sub> capture [34]. It has been observed that adsorbents that change with chemical reagents have boosted the CO<sub>2</sub> sorption capacity; for example, chemical modification with K<sub>2</sub>CO<sub>3</sub> has significantly increased CO<sub>2</sub> adsorption capacity for two hydrotalcite-like compounds at 400 °C [35]. Using these modified HTICs, CO<sub>2</sub> adsorption values in the 0.9 mol/kg range are obtained. This improvement could be attributed partly to CO<sub>2</sub> absorption by the chemically changed material [36].

Dolomites, silicates, and synthetic absorbent materials have been employed to change the balance of hydrocarbon steam reforming toward H<sub>2</sub> creation via selective CO<sub>2</sub> removal from the system [37]. Some of the most common CO<sub>2</sub> removal techniques are cryogenic separation, dry adsorption, wet absorption, and membrane separation. However, the power inputs required are rather high, making the benefits in terms of total CO<sub>2</sub> emissions insignificant [38]. Materials/technologies were developed/adopted for CO<sub>2</sub> capture/separation; some are discussed with their advantages and disadvantages in Figure 1.

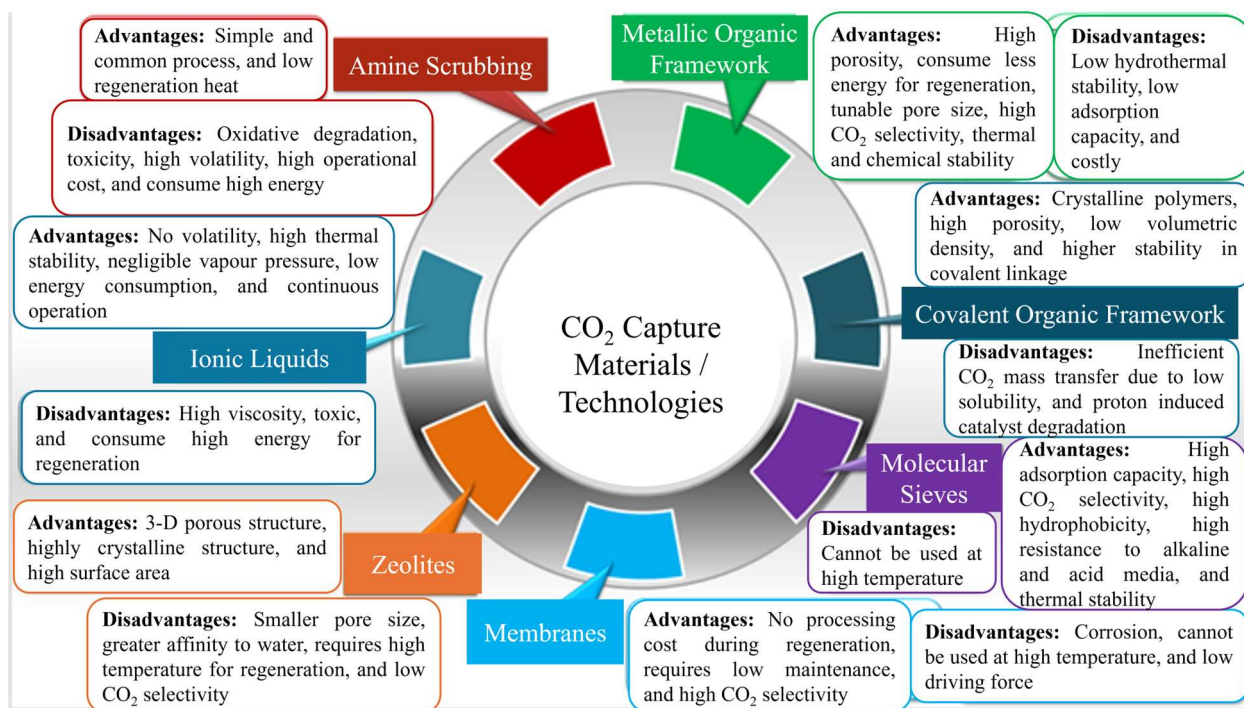


**Figure 1.** Various materials/technologies developed/adopted for CO<sub>2</sub> capture.

### 2.1. CO<sub>2</sub> adsorption techniques used in industries

Adsorption of CO<sub>2</sub> from industrial sources is a critical focus area in efforts to mitigate greenhouse gas emissions. Extensive research has been undertaken over the last few decades for the development of strategies for CO<sub>2</sub> adsorption from various sectors [39]. Carbon dioxide adsorption techniques play a crucial role in various industries, particularly in addressing environmental concerns and complying with emission regulations. Several methods are employed for CO<sub>2</sub> adsorption, and some commonly used techniques in industries are discussed in Table 1 with their advantages and limitations.

**Table 1.** Various techniques used in the industries for CO<sub>2</sub> adsorption.

No.	Techniques for CO <sub>2</sub> adsorption	Advantages	Limitations	Ref.
1.	Amine scrubbing	<ul style="list-style-type: none"> <li>Stable operation</li> <li>Good reactivity</li> <li>High capacity</li> </ul>	<ul style="list-style-type: none"> <li>Consume High energy (approximately 30 % to run a power plant)</li> <li>Low capacity (CO<sub>2</sub> capture)</li> <li>High loss of solvent due to evaporation</li> <li>Poor thermal stability</li> <li>Equipment corrosion</li> </ul>	[40]
2.	Pressure swing adsorption (PSA)	<ul style="list-style-type: none"> <li>Stability</li> <li>Lower energy requirements</li> <li>Versatility</li> <li>Scalability</li> </ul>	<ul style="list-style-type: none"> <li>Adsorbent degradation</li> <li>High capital cost</li> <li>More space requirement</li> <li>Complexity in integration</li> </ul>	[41]
3.	Temperature swing adsorption (TSA)	<ul style="list-style-type: none"> <li>Lower energy requirements</li> <li>Applicability to various gas streams</li> <li>Lower operating cost</li> <li>Flexible in adsorbent materials</li> </ul>	<ul style="list-style-type: none"> <li>Heat integration challenges</li> <li>Complex Engineering</li> <li>Adsorbent stability</li> <li>Limited to small scale industries</li> </ul>	[42]
4.	Solid sorbent (like MOF)	<ul style="list-style-type: none"> <li>High CO<sub>2</sub> capture capacity</li> <li>Flexibility in design</li> <li>Reduced corrosion issues</li> <li>Low energy consumption</li> </ul>	<ul style="list-style-type: none"> <li>Aging and stability</li> <li>High cost</li> <li>Scale up challenges</li> </ul>	[43]
5.	Membrane separation	<ul style="list-style-type: none"> <li>Energy efficiency</li> <li>Selective separation</li> <li>Continuous operation</li> </ul>	<ul style="list-style-type: none"> <li>Material durability</li> <li>Limited applicability to high CO<sub>2</sub> concentrations</li> <li>Limited to gas streams</li> </ul>	[1]
6.	Ionic liquids	<ul style="list-style-type: none"> <li>Environment friendly</li> </ul>	<ul style="list-style-type: none"> <li>The viscosity of IL is forty times higher than that of aqueous alkanolamine solutions</li> <li>Which brought a great influence on the CO<sub>2</sub> absorption capacity and rate of the absorption of IL</li> </ul>	[44]
7.	CO <sub>2</sub> capture with supported ionic liquids membranes (SILM)	<ul style="list-style-type: none"> <li>Better absorption efficiency</li> </ul>	<ul style="list-style-type: none"> <li>Leaching of the liquid is required through membrane pores when the pressure drops</li> </ul>	[45]
8.	Cryogenic separation	<ul style="list-style-type: none"> <li>Used to capture CO<sub>2</sub> at extremely low temperature</li> </ul>	<ul style="list-style-type: none"> <li>High energy consumption</li> <li>High equipment cost</li> <li>Limited applicability to low CO<sub>2</sub> concentration</li> </ul>	[46]

The mentioned methods/technologies have been applied for CO<sub>2</sub> capture/separation in industries. Although, these methods are good enough for capturing CO<sub>2</sub>, the development of new materials and methods is ongoing to overcome the limitations of the processes mentioned in Table 1. Among the discussed methods/materials, the solid sorbent method has been pointed as one of the efficient techniques to capture CO<sub>2</sub>.

## 2.2. Carbon-based absorbent for CO<sub>2</sub> capture

Carbon-based absorbents are materials that contain carbon and are designed to capture CO<sub>2</sub> from gas streams. These materials typically have high surface areas and can adsorb CO<sub>2</sub> through physical

or chemical interactions. Here are some common carbon-based absorbents used for CO<sub>2</sub> capture [47]. Table 2 shows the advantages and limitations of carbon-based absorbent for CO<sub>2</sub> capture.

**Table 2.** Various carbon-based absorbents for CO<sub>2</sub> adsorption.

No.	Carbon-based absorbent	Advantages	Limitations	Ref.
1.	Activated carbon	<ul style="list-style-type: none"> <li>▪ Highly porous material</li> <li>▪ High surface area</li> <li>▪ Availability of raw materials</li> <li>▪ Compatibility with flue gas</li> </ul>	<ul style="list-style-type: none"> <li>▪ Moderate adsorption capacity</li> <li>▪ Temperature sensitivity</li> <li>▪ Regeneration energy requirement</li> </ul>	[48]
2.	Carbon nanotubes	<ul style="list-style-type: none"> <li>▪ High surface area</li> <li>▪ Tunable pore size</li> <li>▪ Rapid adsorption and desorption kinetics</li> </ul>	<ul style="list-style-type: none"> <li>▪ Synthesis challenges</li> <li>▪ High capital cost</li> <li>▪ Mechanical integrity</li> </ul>	[49]
3.	Graphene-based materials	<ul style="list-style-type: none"> <li>▪ High surface area</li> <li>▪ Tunable properties</li> <li>▪ Lightweight nature</li> <li>▪ conductivity</li> </ul>	<ul style="list-style-type: none"> <li>▪ Aggregation tendency</li> <li>▪ Specific functionalization challenges</li> <li>▪ Health and safety considerations</li> </ul>	[50]
4.	Biochar	<ul style="list-style-type: none"> <li>▪ Renewable and sustainable</li> <li>▪ Chemical stability</li> <li>▪ Agricultural benefits</li> </ul>	<ul style="list-style-type: none"> <li>▪ Low adsorption capacity</li> <li>▪ Regeneration challenges</li> <li>▪ Transport and handling</li> </ul>	[51]
5.	Carbon molecular sieves	<ul style="list-style-type: none"> <li>▪ Tunable pore size</li> <li>▪ Applicability to high-pressure environment</li> <li>▪ High selectivity</li> </ul>	<ul style="list-style-type: none"> <li>▪ Production complexity</li> <li>▪ Limited temperature range</li> <li>▪ Material degradation</li> </ul>	[52]

### 3. Metal-organic frameworks (MOFs) for CO<sub>2</sub> capture

The choice of a MOF for CO<sub>2</sub> capture depends on factors such as pore size, chemical composition, and stability [53]. Some MOFs exhibit a high affinity for CO<sub>2</sub> due to their porous nature and the presence of specific functional groups within the framework. For instance, MOFs studied for CO<sub>2</sub> capture include ZIF-8, HKUST-1, UiO-66, and MIL-101. These MOFs have demonstrated promising results in terms of adsorption capacity and selectivity for CO<sub>2</sub> [54].

ZIF-8 stands out among MOFs due to its remarkable stability, tunable pore size, and large surface area. Its high stability ensures structural integrity across conditions, while the ability to adjust pore dimensions enables selective gas adsorption [55]. The simplicity of its synthesis process, coupled with cost-effectiveness, enhances its practicality for industrial applications. The materials used for its synthesis can be economically advantageous [56]. Overall, ZIF-8's unique combination of properties, including ease of synthesis, tunable structure, and adaptability to various applications, positions it as a promising MOF with distinct advantages over others in gas storage, separation, and catalysis. Table 3 shows the comparison of key MOFs for gas storage, separation, and catalysis.

Over the past two decades, research on ZIF-8 has undergone remarkable advancements, particularly in its application for CO<sub>2</sub> capture. The unique properties of ZIF-8, including high porosity, tuneable structure, and exceptional chemical stability, have made it an attractive material for gas separation and storage.

**Table 3.** Comparison of key MOFs for gas storage, separation, and catalysis.

MOF	Pore size (nm)	Surface area (m <sup>2</sup> /g)	CO <sub>2</sub> uptake (mmol/g)	Selectivity (CO <sub>2</sub> /N <sub>2</sub> )	Thermal stability (°C)	Chemical stability
ZIF-8	0.34	1200–1600	0.88–1.62	Moderate	~550	High
MOF-74	0.98	1000–1400	8.4–9.5	High	~350	Moderate
HKUST-1	0.9	700–1500	4.5–5.2	Moderate	~350	Low (sensitive to moisture)
UiO-66	0.8	1000–1400	3.4–4.0	High	~500	Very high
MIL-101	1.2–2.9	3000–4000	8.2–9.6	High	~275	Moderate

To provide a comprehensive view of the evolution of ZIF-8 research, a graphical timeline (Figure 2) is presented, summarizing major breakthroughs in the field. These milestones include the synthesis of ZIF-8, its molecular sieving properties, membrane integration, surface modifications, composite development, and direct air capture applications.

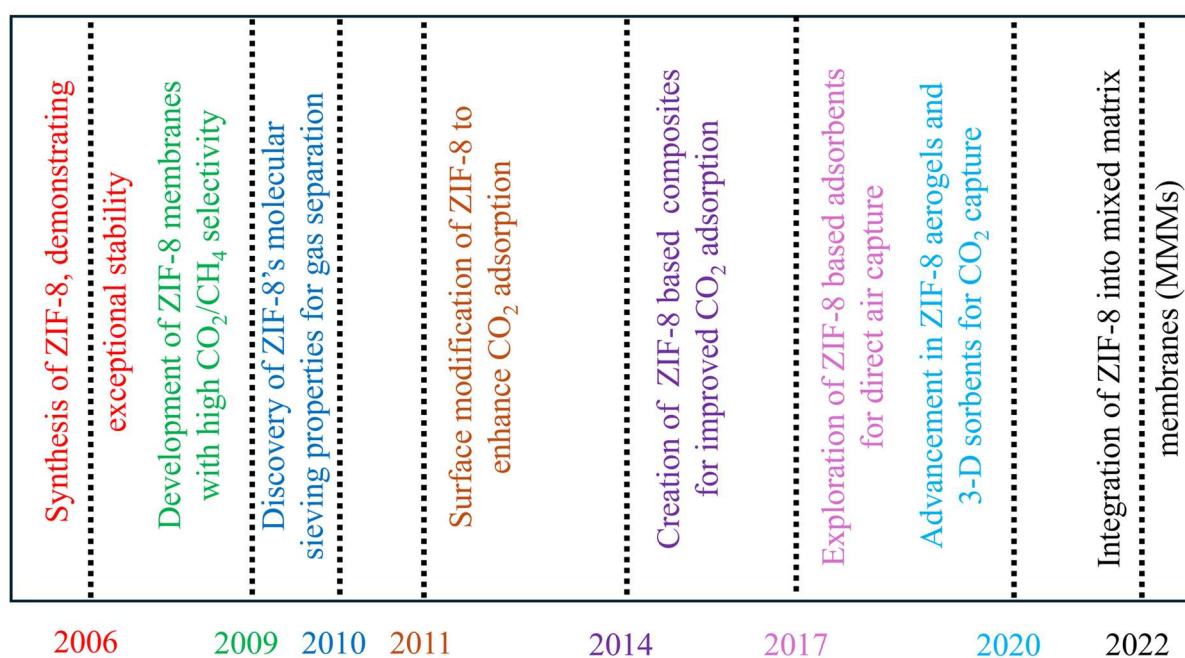
**Figure 2.** Timeline of major breakthroughs in ZIF-8 research for CO<sub>2</sub> capture, showcasing key developments in synthesis, adsorption, membrane integration, and industrial applications.

Figure 2 illustrates the significant progress in utilizing ZIF-8 for CO<sub>2</sub> separation, highlighting key achievements that have shaped the research landscape. The timeline underscores how continuous improvements in synthesis methods, functionalization, and composite integration have enhanced the adsorption efficiency, permeability, and selectivity of ZIF-8-based materials for CO<sub>2</sub> capture applications.

With increasing global concerns over rising CO<sub>2</sub> levels, direct air capture (DAC) has gained attention as a viable strategy for reducing atmospheric CO<sub>2</sub> concentrations. Unlike conventional capture methods that focus on industrial flue gases, DAC operates at ultra-dilute CO<sub>2</sub> levels (~400 ppm), making the development of highly selective and efficient adsorbents essential. MOFs, particularly

ZIF-8 and its derivatives, have emerged as promising materials for DAC due to their high porosity, tuneable surface chemistry, and selective CO<sub>2</sub> adsorption properties [47].

Among MOFs, ZIF-8 exhibits exceptional thermal and chemical stability, making it an attractive choice for low-concentration CO<sub>2</sub> capture applications. However, its hydrophobic nature and pore aperture (~0.34 nm) present challenges in adsorbing CO<sub>2</sub> under ambient conditions. To enhance DAC performance, researchers have explored ligand modifications and functionalized ZIF-8 derivatives, improving CO<sub>2</sub> affinity through amine-functionalization and pore engineering [23,24]. Furthermore, ZIF-8-based composite sorbents and hybrid membranes have demonstrated enhanced selectivity and faster adsorption kinetics, making them more efficient for air purification and carbon capture applications.

Beyond ZIF-8, other MOFs such as HKUST-1, UiO-66, and MOF-74 have been studied for DAC applications, with MOF-74 showing particularly high CO<sub>2</sub> uptake at low pressures. Studies also indicate that MOF-based solid sorbents, when integrated with monolithic supports or structured adsorbents, can significantly reduce energy costs and enhance CO<sub>2</sub> removal efficiency in DAC systems. As research advances, the optimization of MOF-based materials continues to focus on improving CO<sub>2</sub> uptake capacity, stability, and regeneration efficiency, ensuring their practical viability in large-scale direct air capture applications [19–24].

#### 4. Various routes to synthesize ZIF-8

ZIF-8 has been synthesized using various methods, some of which are briefly mentioned below.

##### 4.1. Solvothermal method

The solvothermal synthesis route has been used to synthesize high-quality single-crystal ZIF-8 [57]. The simplicity and low-temperature are very suitable for mass production [11]. The main disadvantage of this technique is the extensive ZIF-8 macro crystal preparation [58]. In this approach, ZIF-8 was prepared using two solvent systems: dimethylformamide (DMF) and methanol (MeOH). A total of 2 mmol of zinc nitrate hexahydrate (Zn (NO<sub>3</sub>)<sub>2</sub>·6H<sub>2</sub>O, 98%), 2-methylimidazole (MeIM, 98%), and N,N-dimethylformamide were suspended in 50 mL of N,N-dimethylformamide (DMF, industrial grade) and rapidly agitated until a clear solution was formed [59]. Following this, the substrate mixture was transferred to a 100 mL Duran bottle with a Teflon taped screw cap, and the solution was heated in a convection oven at 140 °C for 24 h [60]. The product was filtered, washed with DMF several times, kept in MeOH for 3 days, and dried at room temperature (Figure 3). The same composition of the precursors was mixed in 80 mL of methanol (MeOH), which was left at room temperature for 24 h without stirring, to prepare ZIF-8 using methanol solvent. The product was washed several times with MeOH, centrifuged, and dried overnight in a vacuum oven at room temperature. The dried powder was collected for characterization.



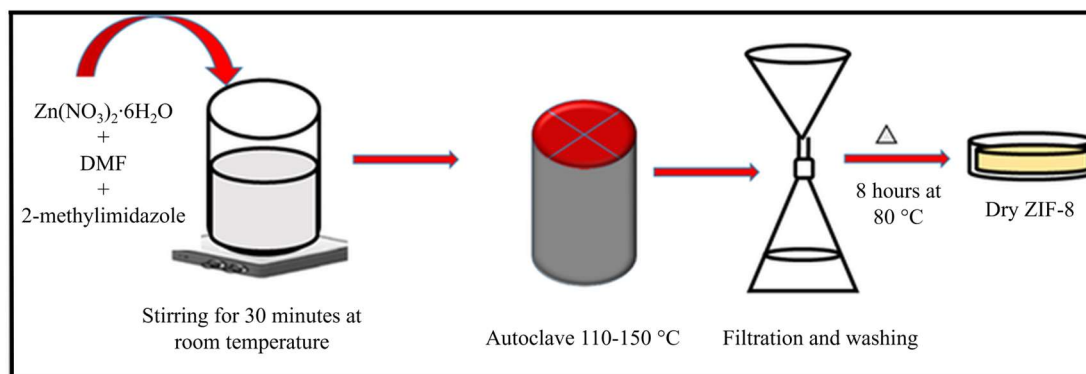


**Figure 3.** Synthesis of ZIF-8 via the solvothermal method.

#### 4.2. Microwave-assisted method

The microwave-assisted method is a solvent-free route to synthesize ZIF-8 particles. In this route, synthesis is completed in  $\sim 4$  h, which is five times less than the conventional synthesis route [61]. The ZIF-8 obtained by this method has a large surface area and microprobe volume compared to those produced by a conventional method. The main disadvantage of this route is its processing temperature, due to which a large particle size ZIF-8 is produced [62]. The nucleation and crystallization have been enhanced at a higher temperature, which increases the particle size of the produced ZIF-8 [63]. The microwave-assisted method is similar to the solvothermal synthesis route except for the temperature and time for the autoclave. In this method, 17 mL of the substrate mixture obtained from the solvothermal method (DMF) was put into a 35 mL tube, sealed with a septum, and placed in a microwave oven (Discover S-class, CEM, Maximum power is 300 W). The resulting mixture was heated to 120–160 °C at 80 W, held for 3 h, and then cooled to room temperature [64]. The dark yellow powder was separated by centrifuging. The product was washed with DMF several times and dried at 100 °C (Figure 4).

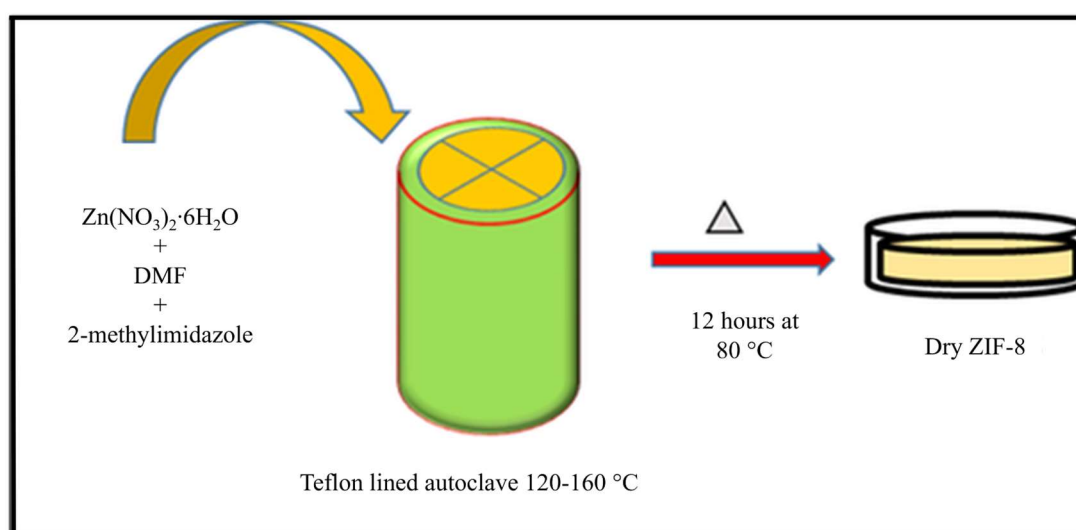


**Figure 4.** Schematic diagram represents the synthesis of ZIF-8 via the microwave-assisted method.

### 4.3. Sonochemical method

Sonochemical synthesis is based on applying high-energy ultrasound to a reaction mixture. Ultrasound in this synthesis is applied to speed up chemical reactions [65]. The ZIF-8 produced by the sonochemical route has a small particle size and narrow particle distribution. This method can be applied for mass production due to its short time processing compared to the traditional method [66]. Although, this method is advantageous for industrial applications, this technique has certain limitations: The reaction parameters can be more effectively controlled before being used in systematic studies of MOFs [67]. The synthesis of ZIF-8 by the sonochemical route can be done using  $\text{Zn}(\text{NO}_3)_2 \cdot 6\text{H}_2\text{O}$  and triethylamine as precursors. Initially, 0.67 g (2 mmol) of  $\text{Zn}(\text{NO}_3)_2 \cdot 6\text{H}_2\text{O}$  and 0.167 g (2 mmol) of MeIM were mixed in 50 mL of DMF and stirred until a clear solution was obtained. Then, 0.5 mL of triethylamine (TEA,  $(\text{C}_2\text{H}_5)_3\text{N}$ , 99%) was added. The obtained mixture was then transferred to a 70 mL horn-type custom-made reactor and connected to a sonicator bar (VCX500, 500 W at 20 kHz) for 1 h. After the synthesis at 60% power, the sample was washed with DMF three times and placed in methanol, which was decanted and replenished four times for 48 hrs. After filtration, the sample was dried in a vacuum oven at 80 °C [55]. The powder was then collected for further characterization (Figure 5).

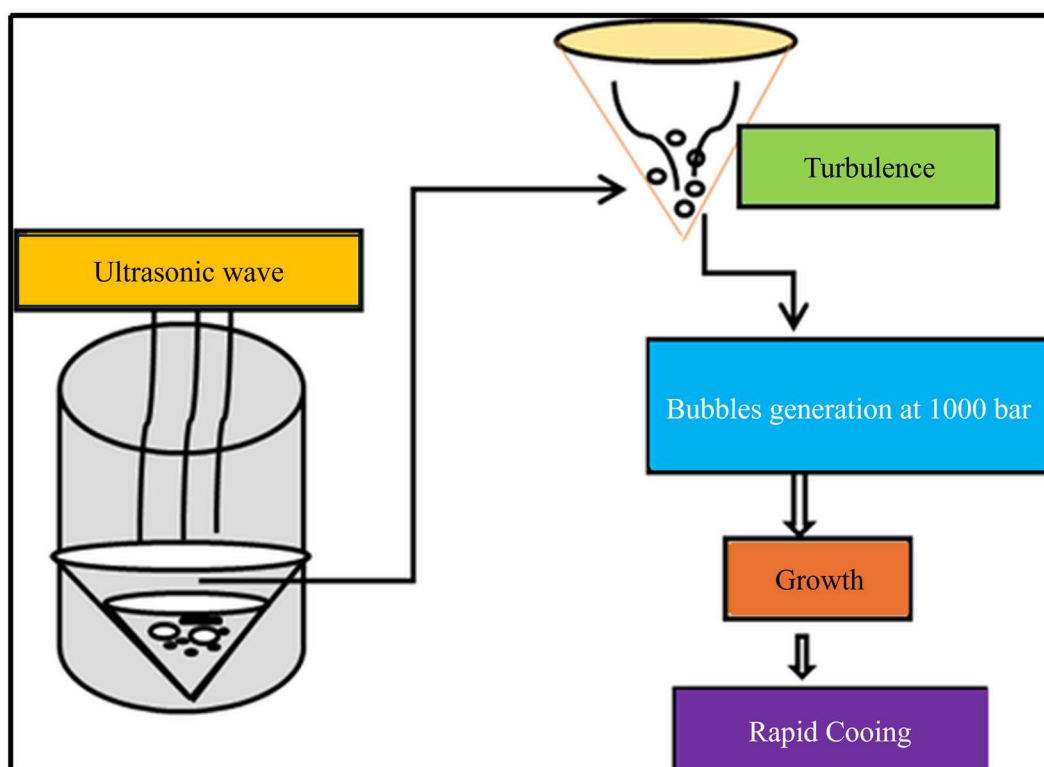


**Figure 5.** Synthesis of ZIF-8 via the Sonochemical method.

### 4.4. Mechanochemical method

In this method (Figure 6), grinding or mechanochemical force can be used to initiate chemical reactions by mechanically breaking chemical bonds, which is then followed by some chemical change [68]. Pichon et al. [69] studied this route in 2006 in their solvent-free approach to MOF synthesis. In this

route, metal, salt, and the ligand are ground together for a few minutes without using any heat, resulting in the formation of the MOF [70]. One of the most important reasons is the method's environmental benefit, which enables large-scale green production while avoiding using large quantities of unpleasant solvents [71]. This makes it safer than the traditional solvothermal route, which employs organic solvents and high temperatures. Furthermore, the absence of solvent molecules in the framework or pores of the MOF structures is advantageous [72]. The reaction times are also typically very short, ranging from 10 to 60 min, which is significantly less than the solvothermal synthesis procedures. Furthermore, the material is subjected to physical grinding conditions, forming small fragments from large particles. This process offers readily compact nano-MOFs [73]. While employing this strategy, it is crucial to ensure the reaction's completion, retain the original MOF's established pore metrics (size, shape, and distribution), and apply a mechanical force consistently throughout the reaction mixture [74]. This process has challenges with reproducibility because the uniformity of the acquired crystal's size and shape varies greatly depending on the strength and length of the grinding [75]. ZIF-8 was synthesized using zinc oxide and ammonium nitrate as a precursor. Initially, a 25 cm<sup>3</sup> steel jar with five 10 mm-diameter steel ball bearings was filled with 0.064 g (0.79 mmol) of zinc oxide (ZnO, 99.9%), 0.128 g (1.56 mmol) of MeIM, and 0.020 g (0.25 mmol) of ammonium nitrate (NH<sub>4</sub>NO<sub>3</sub>, 98%, Sigma-Aldrich). The combination was milled for 45 min at 25 Hz in the Retsch MM200 mill. The product was washed three times with DMF and MeOH before being dried in a vacuum oven at room temperature [76]. The product was dried and collected for further characterization.

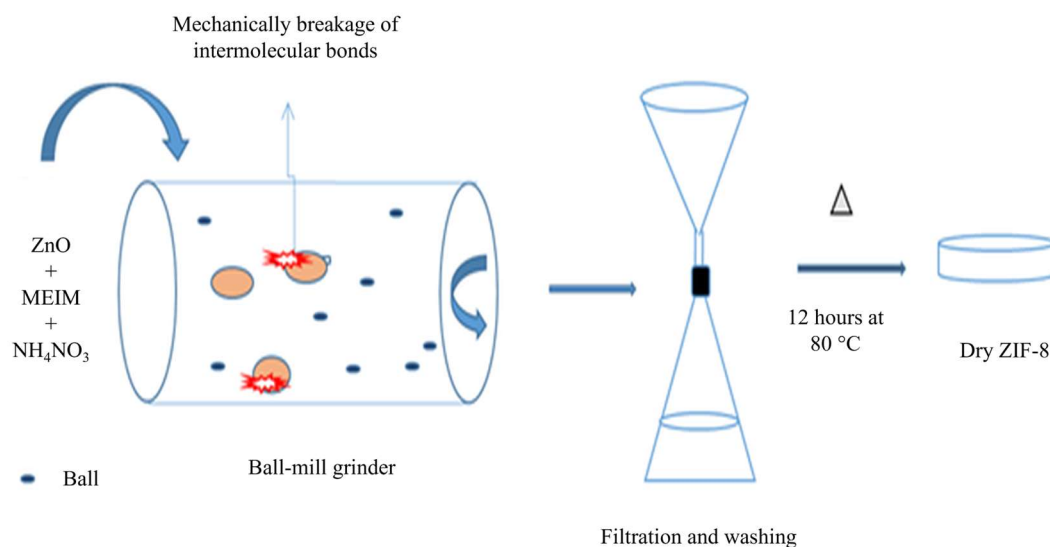


**Figure 6.** Synthesis of ZIF-8 via the mechanochemical method.

#### 4.5. Dry-gel conversion (DGC) method

In this route, materials were placed on a sieve or porous support on top of an autoclave container, with a small amount of solvent at the bottom [77]. The solvent can be recovered with little contamination and reused for subsequent reaction runs by separating the solvent and reactant mixture [78]. Solvent reuse is important because the industry prefers such environmental and economic improvements in product synthesis. Other advantages of DGC techniques include lower solvent amounts, higher yields, and a smaller reactor size [79]. Initially, 0.11 g (0.5 mmol) of zinc acetate

dehydrate ( $\text{Zn}(\text{OAc})_2 \cdot 2\text{H}_2\text{O}$ , 99%) was mixed with 0.41 g (5 mmol) of MeIM. The mixture of substrates was placed on a holed Teflon-plate inside a 30 mL Teflon-lined stainless-steel autoclave.  $\text{H}_2\text{O}$  (2.0 mL) was added at the bottom of the autoclave, and the assembly was heated at 120 °C for 24 h. After the reaction, the autoclave was rapidly cooled in cold water, and the light yellow-colored product from the Teflon-plate inside the autoclave was separated by filtration and washed with  $\text{H}_2\text{O}$  three times [80]. Finally, it was dried in a vacuum at 150 °C for 6 h [81]. The sample was dried and collected for further characterization (Figure 7).

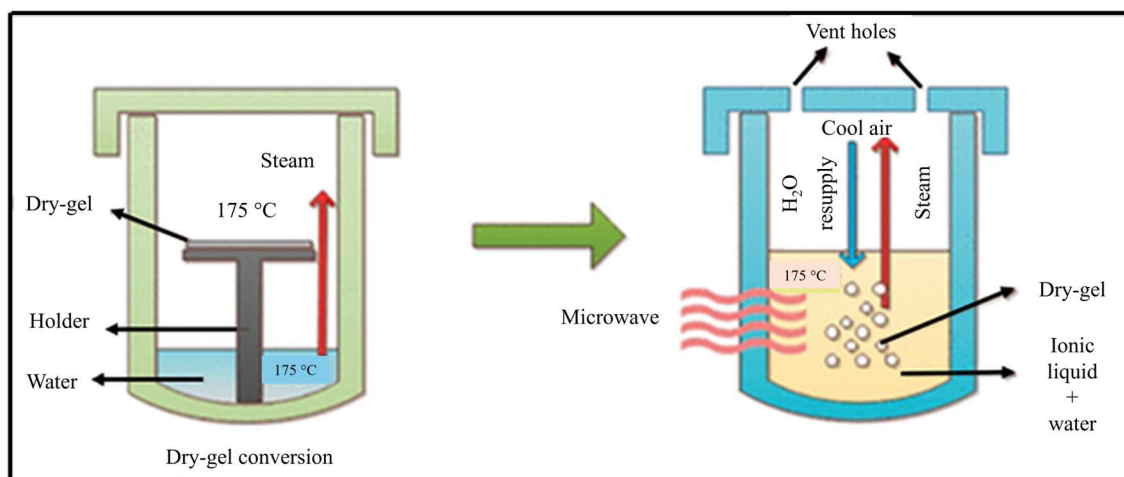


**Figure 7.** Synthesis of ZIF-8 via the microwave-assisted dry-gel conversion method.

#### 4.6. Microfluidic synthesis method

In microfluidic synthesis, continuous-flow micro reactors have been used for the production of nanoparticles with narrow size distributions due to their precise reaction control [82]. In this method, the  $\text{Zn}(\text{NO}_3)_2$  (669 mg, 2.25 mmol) and MeIM (12.930 g, 157.5 mmol) were separately prepared in 45 mL deionized (DI) water and then transferred using a syringe pump to a T-junction in the reactor setup [83], where the substrate solution droplets were formed in a continuous flow of fluorinated oil (Figure 8) [84]. The substrate solution droplets surrounded by oil entered a 1/16-inch tube and extended through an oil bath at 150 °C. The flow rates for both solution and oil were adjusted to  $0.5 \text{ mL h}^{-1}$ . ZIF-8 crystals separated from the oil phase were washed with DMF three times and once with methanol [85]. The filtered product was dried before it was subjected to further characterization. The microfluidic synthesis route (similar chemicals and procedures) has also been used by researchers in their work [86–88].

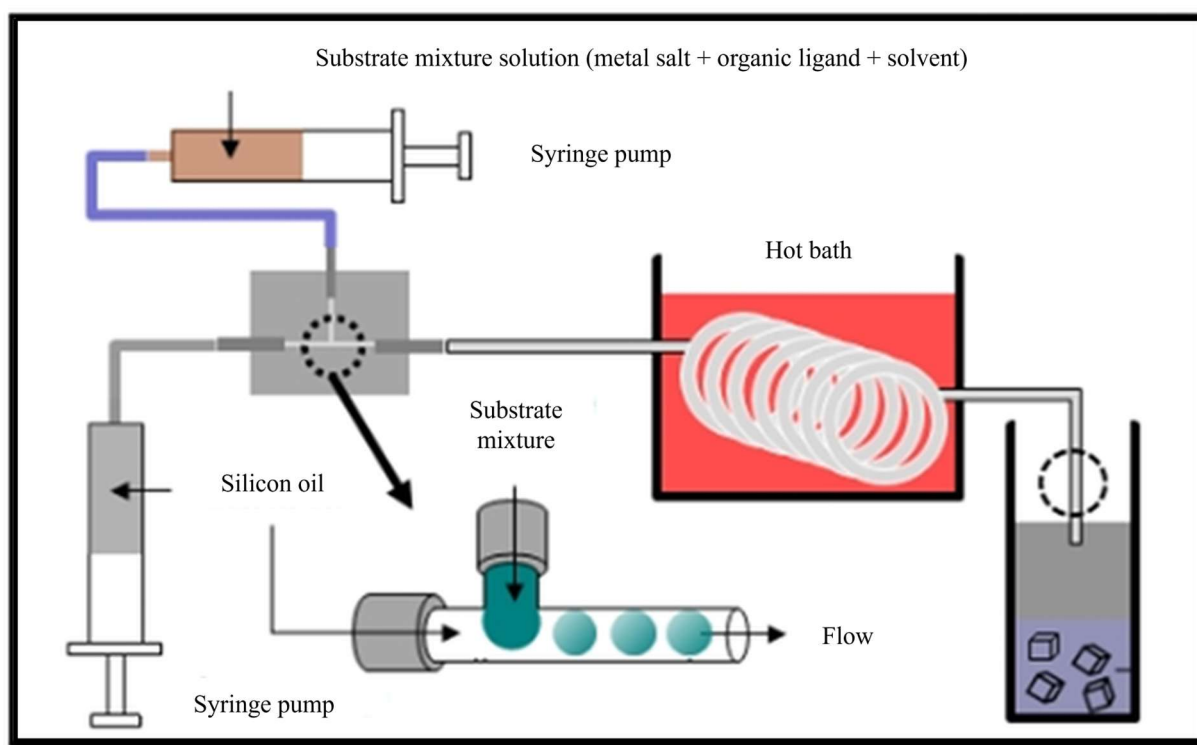


**Figure 8.** Schematic representation of the micro fluidic method for ZIF-8 synthesis.

#### 4.7. Hydrothermal method

The hydrothermal method is a low-cost and ecologically benign method of producing ZIF-8 crystals [89]. This method replicates synthesis by simulating chemical processes in an aqueous solution at temperatures above the boiling point of water [90]. Researchers believe that hydrothermal synthesis of coordination frameworks will lead to a shift toward commercial manufacturing at high production rates by lowering associated production costs and environmental consequences. In comparison to the solvothermal approach, this method yields smaller ZIF-8 particles [91]. Zinc nitrate hexahydrate and 2-methyl imidazolate are the key reagents employed in the synthesis. However, hexadecyltrimethylammonium chloride (CTAC), trimethylstearyl ammonium chloride (STAC), sodium dodecyl sulfate, cetyltrimethylammonium bromide (CTAB), and tetrapropylammoniumbromide (TPABr) are the surfactants used [92]. The stoichiometric amounts of zinc salt and 2-methylimidazole were first dissolved in separate beakers of DI water. In a typical synthesis, 0.29 g of zinc nitrate hexahydrate was first dissolved in 10 mL DI water (solution A), followed by 4.54 g of 2-methylimidazole in 70 mL DI water (solution B), and whenever possible, the surfactant was dissolved in solution B first. Solution A was swiftly poured into solution B, which was agitated at 300 rpm in a larger beaker, and these two solutions were allowed to react at a specific temperature for a certain period. Following the completion of the synthesis, the products were collected by repeated centrifugation (8000 rpm, 30 min), washed three times with DI water and methanol, and dried [93]. The schematic representation of hydrothermal method for ZIF-8 is shown in Figure 9.

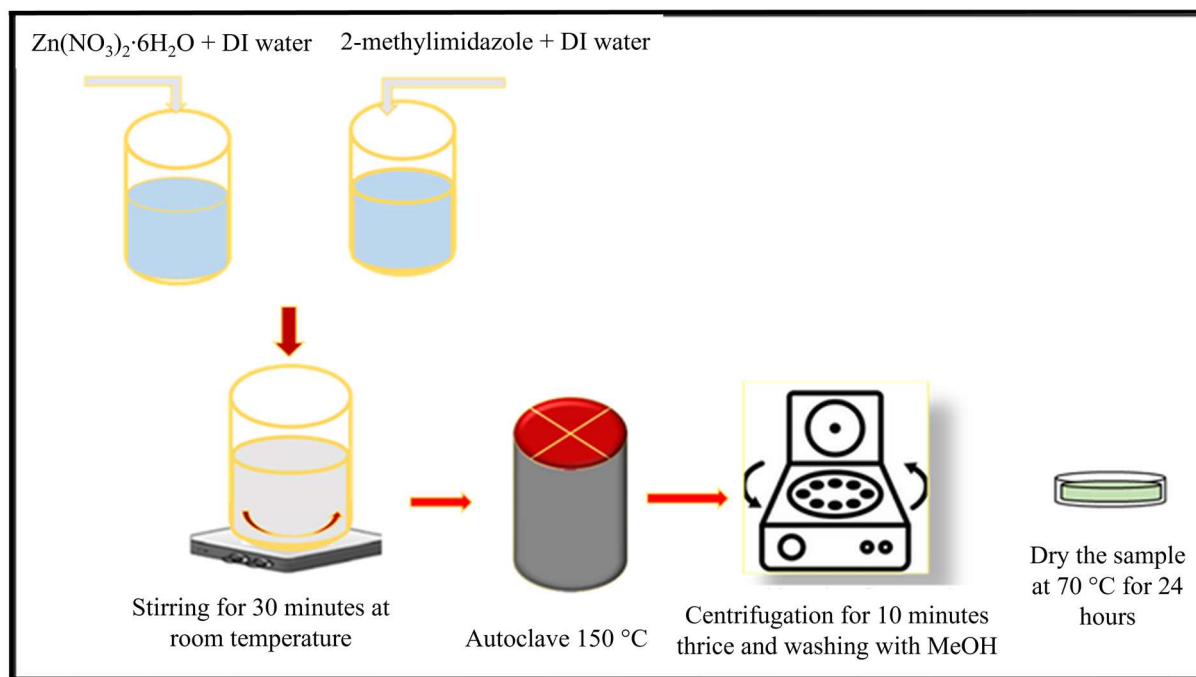


**Figure 9.** Schematic representation of the hydrothermal method for ZIF-8 synthesis.

#### 4.8. Rapid synthesis of ZIF-8

This is a non-solvothermal route to synthesize ZIF-8 at room temperature. It is a rapid synthesis route (Figure 10) with an easy variation of particle size [94]. Zinc nitrate hexahydrate ( $\text{Zn}(\text{NO}_3)_2 \cdot 6\text{H}_2\text{O}$ , 98%) and 2-Methylimidazole (MeIM, 98%) were employed as precursors for the production of ZIF-8 in this approach. Initially, 1.17 g of  $\text{Zn}(\text{NO}_3)_2 \cdot 6\text{H}_2\text{O}$  and 22.70 g of 2-methylimidazole were dissolved separately in 8 g of zinc nitrate hexahydrate and 80 ml DI water. These two solutions were stirred for 5 min at room temperature, and pH was monitored. The resulting nanoparticle was separated from milky dispersion by centrifugation at 7000 rpm for 5 min. The precipitate was washed with DI water three times. The resulting nanoparticles were dried in an oven overnight at  $85\text{--}90\text{ }^\circ\text{C}$  in a Teflon vessel using an autoclave. These steps were repeated to synthesize ZIF-8 of different particle sizes by varying stirring time from 5 to 60 min and at different pH values at room temperature. Extensive experimentation would be required by attempting different combinations to find the most suitable method, particle size, and structure of ZIF-8 [11,23,95].

This method has advantages over the mentioned methods because the particle size of synthesized ZIF-8 can easily vary. The particle size of ZIF-8 is an influential parameter in capturing/adsorbing the  $\text{CO}_2$ . A comparative analysis of advantages and limitations of all synthesis routes are shown in Table 4. Table 5 presents the quality assessment matrix for ZIF-8 based on synthesis parameters.



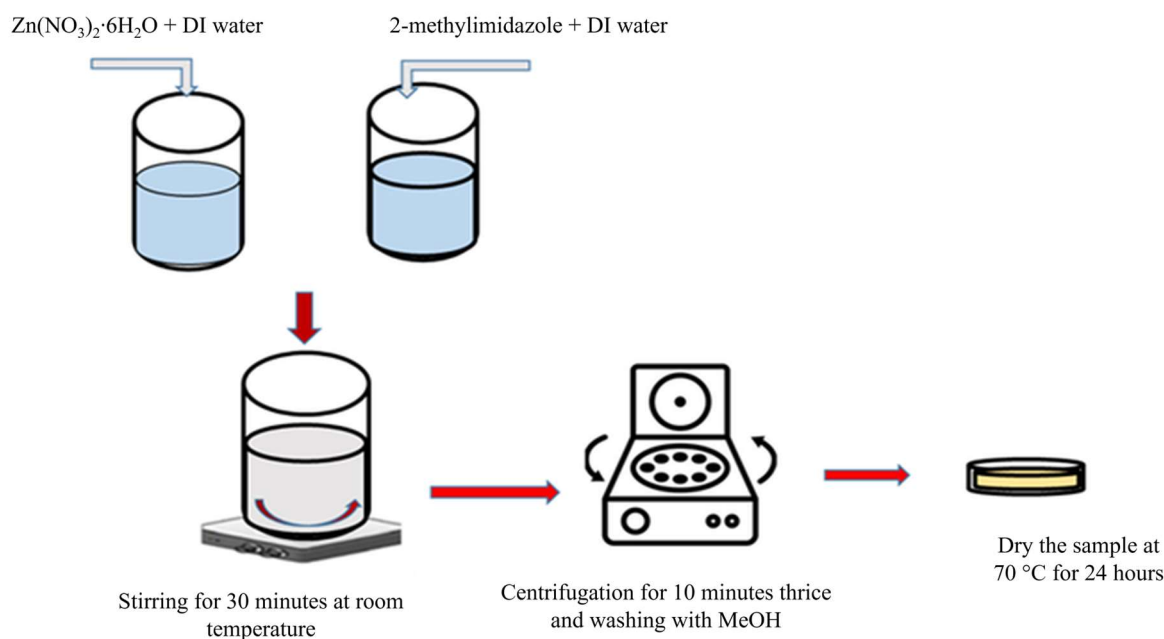


**Figure 10.** Schematic representation of the rapid synthesis of ZIF-8.

**Table 4.** Advantages and limitations of different ZIF-8 synthesis routes.

Synthesis routes	Advantages	Limitations
Solvothermal route	<ul style="list-style-type: none"> <li>High-quality single-crystal</li> <li>Low temperature working</li> <li>suitable for mass production</li> </ul>	<ul style="list-style-type: none"> <li>Macro crystal produced</li> <li>Time-consuming method</li> </ul>
Microwave-assisted	<ul style="list-style-type: none"> <li>Solvent-free synthesis method</li> <li>Less time taken ~4 h</li> <li>Large surfaces are to volume ratio obtain</li> </ul>	<ul style="list-style-type: none"> <li>Control of processing temperature</li> <li>Large particle size obtained</li> </ul>
Sonochemical method	<ul style="list-style-type: none"> <li>Less time consuming</li> <li>Small particle size obtained</li> <li>Useful for industrial application</li> </ul>	<ul style="list-style-type: none"> <li>Control of chemical reaction parameter</li> <li>Setup complication</li> <li>High production cost</li> </ul>
Thermal conductivity	<ul style="list-style-type: none"> <li>Solvent-free synthesis method</li> <li>Less processing time (20–60 min)</li> <li>Nano size particle obtained</li> </ul>	<ul style="list-style-type: none"> <li>Particle size distribution non-uniform</li> <li>Reproducibility issues</li> <li>Precursors are explosive in nature and need more protection</li> </ul>
Dry-gel conversion (DGC) method	<ul style="list-style-type: none"> <li>Lower solvent required</li> <li>High yield obtained at less solvent</li> </ul>	<ul style="list-style-type: none"> <li>Temperature control in a reactor</li> <li>Production cost is high</li> </ul>
Microfluidic synthesis method	<ul style="list-style-type: none"> <li>Size-controlled synthesis of ZIF-8</li> <li>Ecofriendly technique</li> </ul>	<ul style="list-style-type: none"> <li>Lower specific surface area obtained</li> </ul>
Hydrothermal method	<ul style="list-style-type: none"> <li>Smaller particle size obtained compared to the solvothermal route</li> <li>Economically good process</li> </ul>	<ul style="list-style-type: none"> <li>Time-consuming process</li> </ul>
Rapid synthesis route	<ul style="list-style-type: none"> <li>Particle size-controlled synthesis route</li> <li>Less time consuming</li> <li>Easy to vary the particle size</li> <li>Economic and eco-friendly technique</li> </ul>	<ul style="list-style-type: none"> <li>Need extensive research for industrial-scale production</li> </ul>

**Table 5.** Quality assessment matrix for ZIF-8 based on synthesis parameters.

Synthesis route	Morphology	Surface area (m <sup>2</sup> /g)	Crystallinity	Mechanical stability	Gas uptake (CO <sub>2</sub> , N <sub>2</sub> )	Remarks
Solvothermal	Well-defined polyhedral	1200–1600	High	High	Moderate	Standard method, good crystallinity
Hydrothermal	Polyhedral	1000–1400	High	Moderate	Moderate	Water-based, more eco-friendly
Mechanochemical	Irregular	800–1200	Moderate	High	Low	Solvent-free, scalable
Electrochemical	Uniform thin film	1500–1800	High	High	High	Thin film applications
Spray drying	Spherical	900–1300	Moderate	Moderate	Moderate	Suitable for large-scale production
Microwave-assisted	Uniform particles	1300–1700	High	High	High	Rapid synthesis, energy-efficient

## 5. Various routes of ZIF-8 synthesis and their outcomes

The ZIF-8 particles were synthesized using various routes and reported with their outcomes. Table 6 shows the summary of X-ray diffraction (XRD) and scanning electron microscopy (SEM) analyses of ZIF-8 prepared by different routes. The XRD pattern obtained from all the routes is similar, and the highest peak was obtained at  $2\theta = 7.20^\circ$  and (011) plane. It has been reported that ZIF-8 has the ability to absorb CO<sub>2</sub>, N<sub>2</sub>, CH<sub>4</sub>, etc., due to its highly porous structure and larger specific area [96]. It has been reported that water and methanol have been used as solvents in the solvothermal route. The XRD and SEM analyses of ZIF-8 prepared using both (water and methanol) solvents have been similar [97]. However, the structure of ZIF-8 is cubic and hydrangea-like, while using water and methanol as a solvent. ZIF-8s synthesized by the solvothermal route are highly porous but larger and lower the Brunauer, Emmett and Teller (BET) surface area. ZIF-8 produced by microwave-assisted and sonochemical synthesis routes have a smaller particle size compared to those produced by the solvothermal route. However, some of the described synthesis routes (hydrothermal, rapid synthesis, etc.) can produce nano-size ZIF-8s [98,99]. The particle size of ZIF-8 is the influential factor in the preparation of the cellulose filter used to capture CO<sub>2</sub> [100]. Therefore, the preparation of ZIF-8 for CO<sub>2</sub> adsorption/capture is method-specific. Among the described methods, ZIF-8 prepared by rapid synthesis and the hydrothermal route has a smaller particle size than those obtained from other routes [94]. It has been reported that CO<sub>2</sub> uptake by the filters/composites prepared by ZIF-8 obtained from hydrothermal routes is higher than that obtained from other routes due to a small particle size (nano-size), higher pore volume, and specific surface area [11,101]. The ZIF-8 prepared by mechanochemical routes has a rhombic dodecahedron-like structure but a larger particle size compared to those obtained through the hydrothermal and rapid synthesis route. The CO<sub>2</sub> uptake also depends on the structure of ZIF-8. It has been reported that the hexagonal structure of ZIF-8 demonstrates ~52%, 35%, and 65%, CO<sub>2</sub>, N<sub>2</sub>, and CH<sub>4</sub> uptake, respectively [102,103]. In another study, it was reported that the leaf-like structure of ZIF-8 demonstrates ~56% higher CO<sub>2</sub> adsorption than normal ZIF-8. The microwave-assisted route of synthesis has been reported as a solvent-free technique for ZIF-8 synthesis. The ZIF-8s produced using the microwave-assisted synthesis route are hexagonal; however, the BET surface area is lower compared to ZIF-8s obtained from the solvothermal route. The microwave-assisted technique has a complication and it is not cost effective for industrial

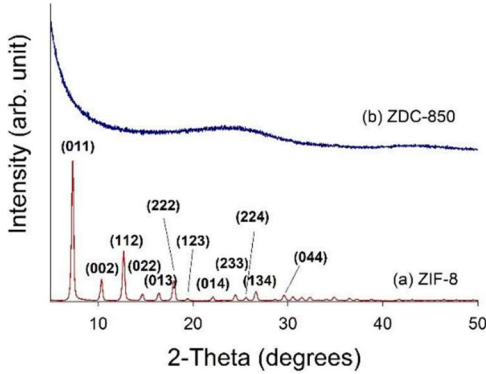
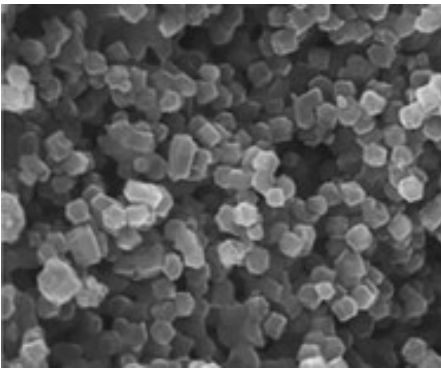
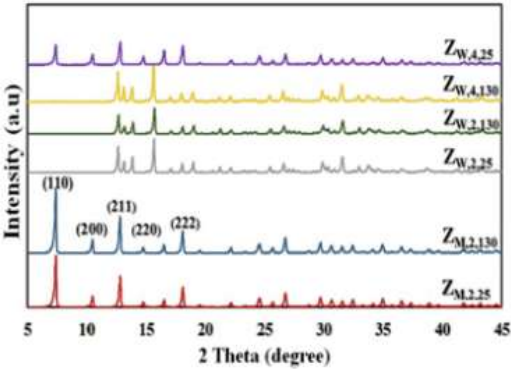
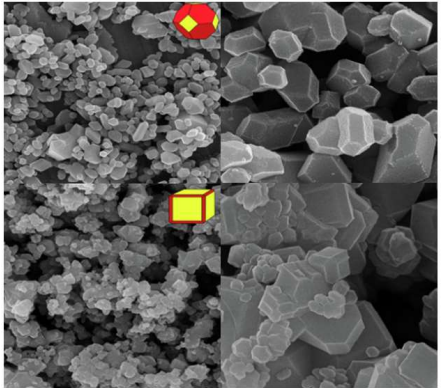


purposes [75]. Overall, it is concluded that the ZIF-8 prepared by rapid synthesis and the hydrothermal route is more efficient (small particle size) than other routes. Enhancing CO<sub>2</sub> adsorption involves choosing the right synthesis route for ZIF-8 and optimizing its particle size. Furthermore, membrane composition and processing also contribute to the improvement of CO<sub>2</sub> adsorption [62].

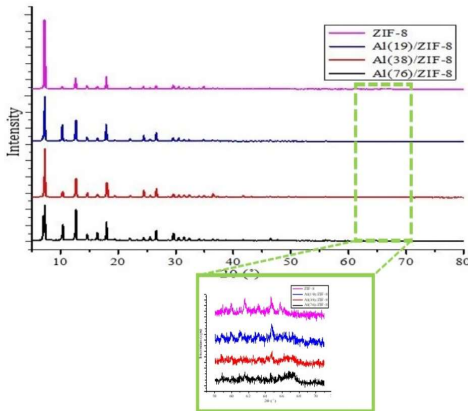
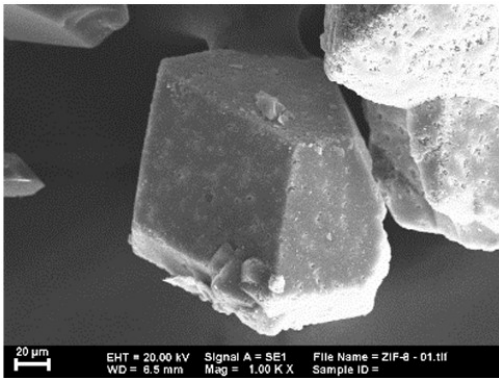
While ZIF-8-based composite membranes and aerogels have emerged as promising materials for CO<sub>2</sub> capture, several challenges hinder their large-scale deployment. One of the primary issues is poor interfacial adhesion between ZIF-8 and polymer matrices in mixed matrix membranes (MMMs), often leading to non-uniform dispersion and defect formation, which adversely affects gas separation performance. Additionally, the fragile nature of ZIF-8 aerogels makes their scalable fabrication complex, as they are highly sensitive to synthesis conditions such as temperature, pressure, and solvent selection. Another critical limitation is the permeability-selectivity trade-off, where membranes with high permeability often suffer from lower selectivity for CO<sub>2</sub> separation, requiring further functionalization and hybridization to enhance efficiency. Moreover, real-world industrial CO<sub>2</sub> capture conditions expose these materials to moisture, impurities (SO<sub>2</sub>, NO<sub>x</sub>), and variable pressure/temperature environments, which may lead to degradation and loss of adsorption capacity over time. Addressing these challenges requires advancements in scalable synthesis techniques, improved polymer compatibility, and cost-effective production routes, all of which are actively being explored to enhance the practical feasibility of ZIF-8 composites and aerogels for industrial CO<sub>2</sub> capture applications.

Table 6 highlights ZIF-8 synthesis methods and their outcomes.

**Table 6.** ZIF-8 synthesis methods and their outcomes.

No.	ZIF-8 route	synthesis	XRD pattern	Morphology (SEM)	Outcome	Ref.
1.	Colloidal chemistry route				<ul style="list-style-type: none"> <li>▪ Average crystal size ~63 nm</li> <li>▪ CO<sub>2</sub> uptake ~0.88 mmol/g</li> </ul>	[104]
2.	Solvothermal method				<ul style="list-style-type: none"> <li>▪ Methanol and water are used as solvent</li> <li>▪ Relative crystallinity was obtained ~0.86 and 0.59 for Z<sub>M,2,130</sub>, Z<sub>M,2,25</sub> and Z<sub>W,4,130</sub>, respectively.</li> </ul>	[97]

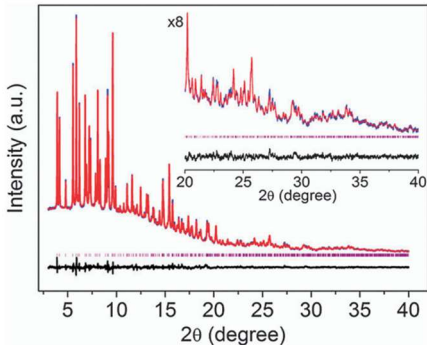
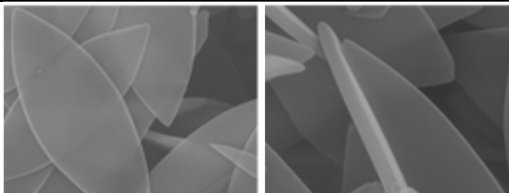
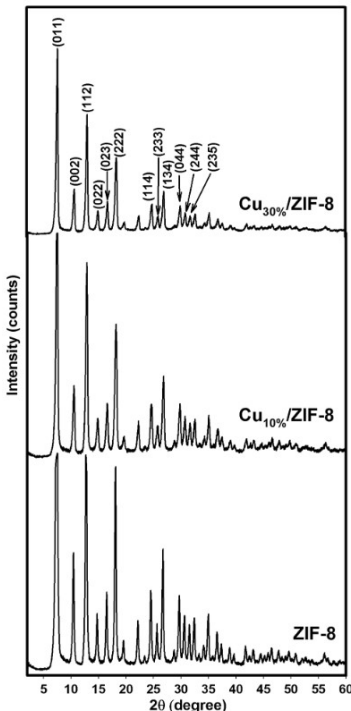
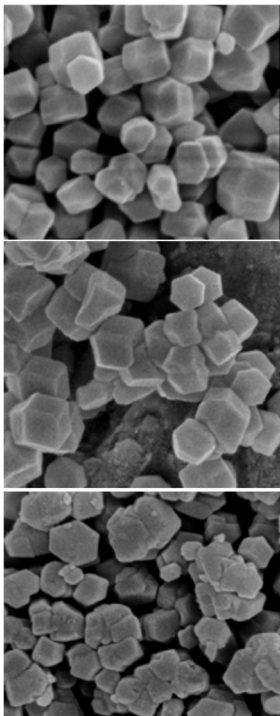
*Continued on next page*

No.	ZIF-8 route	synthesis	XRD pattern	Morphology (SEM)	Outcome	Ref.
3.	Solvothermal method				<ul style="list-style-type: none"> <li>▪ ZIF-8/<math>\text{Al}_2\text{O}_3</math> composite was prepared [105]</li> <li>▪ Sharp cubic structures were obtained due to the incorporation of <math>\text{Al}_2\text{O}_3</math></li> <li>▪ The average pore radius for ZIF-8 has obtained <math>\sim 1.078</math> nm and increases by 16% and 34% with the addition of <math>\text{Al}_2\text{O}_3</math> (38% and 76% by weight), respectively</li> <li>▪ XRD results show slight variation in peaks</li> <li>▪ SEM shows high porosity in ZIF-8</li> </ul>	
4.	Solvothermal method		<p>XRD analysis, on the other hand, provided information on the crystallinity of the ZIF-8 framework. The XRD patterns confirmed that the material had a high degree of crystallinity, indicating that the framework was well-ordered at the atomic level. This level of crystallinity is crucial for ensuring the material's stability and its suitability for high-efficiency applications, such as <math>\text{CO}_2</math> capture. The sharp diffraction peaks in the XRD pattern suggested that the material's structure was well-formed and predictable, which is beneficial for optimizing its gas adsorption properties.</p>	<p>SEM analysis provided detailed insights into the surface morphology and particle distribution of the ZIF-8 material. The SEM images revealed that ZIF-8 exhibited a uniform particle distribution, meaning that the particles were evenly spread across the material without noticeable clumping. This uniformity is essential for ensuring consistent performance in applications like <math>\text{CO}_2</math> capture. The images also indicated that the material possessed a porous, hydrangea-like morphology, which suggests a complex, branched structure, enhancing its surface area and contributing to better gas adsorption efficiency.</p>	<ul style="list-style-type: none"> <li>▪ The average pore size was found to be <math>\sim 1.19</math> nm [59]</li> <li>▪ Porous hydrangea-like morphology</li> <li>▪ Peak intensity was similar to the reported standard data</li> <li>▪ The average particle size of <math>13 \mu\text{m}</math> obtained at <math>140^\circ\text{C}</math></li> <li>▪ A specific surface area of <math>\sim 1045 \text{ m}^2/\text{g}</math> obtained</li> </ul>	

*Continued on next page*

No.	ZIF-8 route	synthesis	XRD pattern	Morphology (SEM)	Outcome	Ref.
5.	Hydrothermal route		XRD analysis, on the other hand, provided critical information about the crystallinity and porosity of the ZIF-8 material. The XRD patterns confirmed that the material had a high surface area, a key feature for effective gas adsorption. Additionally, the XRD results indicated significant porosity, which is essential for the material's ability to adsorb gases like CO <sub>2</sub> . The combination of high surface area and porosity makes ZIF-8 well-suited for CO <sub>2</sub> capture in industrial applications, where efficient gas separation and storage are crucial. The XRD data further demonstrated that the synthesized ZIF-8 maintained its crystalline structure, which is important for ensuring stability and predictable performance in real-world applications.	The SEM analysis revealed the surface morphology of the ZIF-8 material synthesized via the hydrothermal route. The SEM images showed that the ZIF-8 particles exhibited hexagonal and cubic-like shapes, which are characteristic of the material's crystalline structure. These shapes are typical for ZIF-8, as it tends to form well-defined, polyhedral crystals. The particle sizes ranged from 120 to 150 nm, indicating that the material consists of relatively small, well-formed particles. This size range is beneficial for maximizing surface area and optimizing the material for applications such as CO <sub>2</sub> capture, where small particles can enhance the accessibility of the pores for gas adsorption.	<ul style="list-style-type: none"> <li>▪ Hexagonal and cubic-like shape with a size of ~120 to 150 nm</li> <li>▪ Surface area and pore volume of ZIF-8 nanocrystal and cellulose fiber based ZIF-8 filter were ~(1214 m<sup>2</sup>/g, 0.2719 cm<sup>3</sup>/g) and (620.80 m<sup>2</sup>/g, 0.2291 cm<sup>3</sup>/g), respectively</li> <li>▪ CFs@ZIF-8 filter demonstrate 200% higher N<sub>2</sub> adsorption as compare to ZIF-8</li> </ul>	[106]
6.	Microwave-assisted method		XRD analysis of the ZIF-8 crystals confirmed the material's crystallinity and structure, indicating that the microwave-assisted synthesis method resulted in a well-ordered framework. However, the XRD analysis also revealed that the material had a modest CO <sub>2</sub> uptake of about 0.65 mmol/g. This suggests that while the ZIF-8 synthesized by this method does have some ability to adsorb CO <sub>2</sub> , its adsorption capacity is not as high as other materials with higher porosity or optimized surface areas. Nevertheless, the XRD results still highlight the potential utility of this ZIF-8 in gas separation processes, where even modest adsorption capacities can be effective, especially in processes that do not require extremely high volumes of gas adsorption but instead focus on selective and efficient gas capture.	SEM analysis of the ZIF-8 crystals synthesized via the microwave-assisted method revealed that the material had a hexagonal structure, a common characteristic of ZIF-8 crystals. The average size of the crystals was approximately 130 nm, indicating relatively uniform particle dimensions. The smaller size of the particles can be advantageous for maximizing surface area, which plays a crucial role in enhancing gas adsorption properties. The SEM images provide a clear visualization of the crystalline morphology, confirming that the microwave-assisted method successfully produced well-defined crystals. The uniformity and specific shape of these crystals are beneficial for applications like gas separation, where the structure and particle size can directly impact the material's efficiency.	<ul style="list-style-type: none"> <li>▪ The crystal size of ~130 nm was obtained</li> <li>▪ Hexagonal structure obtained</li> <li>▪ CO<sub>2</sub> uptake was ~0.65 mmol/g</li> </ul>	[107]

*Continued on next page*

No.	ZIF-8 route	synthesis	XRD pattern	Morphology (SEM)	Outcome	Ref.
7.	Mechano-chemical method				<ul style="list-style-type: none"> <li>▪ ZIF-8 was synthesized with hexagonal plates and rhombic dodecahedron [108]</li> <li>▪ ZIF-L were obtained in the orthorhombic structure</li> <li>▪ CO<sub>2</sub> uptake for ZIF-L was ~34% higher than ZIF-8</li> </ul>	
8.	Microwave-assisted method				<ul style="list-style-type: none"> <li>▪ The particle size of ~380 nm was obtained [109]</li> <li>▪ The addition of Cu (30 wt.%) in ZIF-8 increases the selective surface area by ~61.5% as compared to ZIF-8</li> <li>▪ The incorporation of Cu does not affect the structure of ZIF-8 because the ionic size of Cu<sup>2+</sup> (0.71 Å) is smaller than that of Zn<sup>2+</sup> (0.74 Å) in tetrahedral coordination.</li> </ul>	

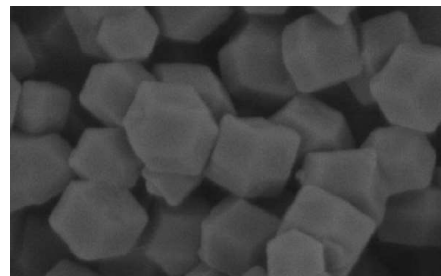
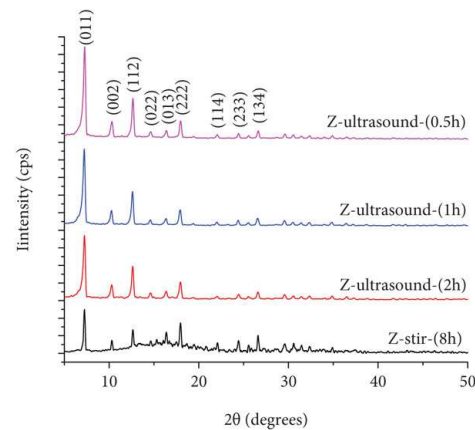
Continued on next page

No.	ZIF-8 route	synthesis	XRD pattern	Morphology (SEM)	Outcome	Ref.
9.	Sono-chemical route		XRD analysis of the sonochemically synthesized ZIF-8 indicated that the material had a substantial pore volume and high surface area, which are crucial factors for efficient gas adsorption. The XRD patterns confirmed that the ZIF-8 maintained a well-ordered crystalline structure, which is essential for ensuring stability and reproducibility in applications. The significant pore volume and surface area highlighted by the XRD data suggest that the material is well-suited for CO <sub>2</sub> adsorption. This is especially important for CO <sub>2</sub> capture, where the efficiency of adsorption directly correlates with the material's porosity and surface area. The robust CO <sub>2</sub> adsorption properties indicated by the XRD analysis underscore the potential of this ZIF-8 material for applications in gas separation and environmental sustainability.	SEM analysis of ZIF-8 synthesized via the sonochemical method revealed that the particles exhibited large sizes, up to 700 nm, which is significantly larger compared to other synthesis methods. The SEM images also highlighted a variation in morphology, particularly influenced by different pH levels during synthesis. Changes in pH can affect the crystallization process, leading to different shapes, sizes, and surface characteristics of the particles. This variability in morphology could result in differing adsorption properties, as the surface area and accessibility of pores are influenced by the particle shape and distribution. The large particle size could potentially limit the overall surface area available for gas adsorption, though the variation in morphology might offer opportunities to optimize the material for specific applications.	<ul style="list-style-type: none"> <li>▪ Large particle size ZIF-8 (700 nm) were prepared</li> <li>▪ Variation of pH seen</li> <li>▪ The highest pore volume (0.60 cm<sup>3</sup>/g) and surface area (1197 m<sup>2</sup>/g) were obtained at a pH of 6.4</li> <li>▪ XRD patterns of each entry confirm the formation of ZIF-8</li> <li>▪ Particle size increases with an increase in pH</li> </ul>	[110]

*Continued on next page*

No.	ZIF-8 route	synthesis	XRD pattern	Morphology (SEM)	Outcome	Ref.
10.	Solvent method		XRD analysis confirmed that the solvent-based synthesis method resulted in a material with an enhanced surface area and pore volume, essential characteristics for effective gas adsorption. The XRD patterns demonstrated that the ZIF-8 crystals maintained a high degree of crystallinity, ensuring structural stability and predictable performance. Additionally, the nitrogen adsorption measurements associated with the XRD data showed values significantly higher than other composites, indicating that the solvent-based synthesis led to a material with a greater capacity for adsorbing gases. This enhanced nitrogen adsorption highlights the superior gas adsorption efficiency of the ZIF-8 material, making it particularly effective for gas separation processes such as CO <sub>2</sub> capture, where large surface area and high porosity are crucial for performance.	SEM analysis of ZIF-8 synthesized using a solvent-based method revealed that the crystals had an average size of 100 nm, which indicates relatively small and uniform particles. This size is beneficial for optimizing surface area, which is crucial for enhancing gas adsorption properties. The SEM images provided clear visual evidence of the crystal structure and morphology, which in this case, appeared consistent with typical ZIF-8 formation. The smaller particle size also suggests that the material could have more exposed surface area, improving its efficiency for applications like gas separation and storage, where high surface area is key to maximizing interaction with gas molecules.	<ul style="list-style-type: none"> <li>▪ The crystal size of ~100 nm was obtained by adding additives [111]</li> <li>▪ ZIF-8 demonstrates higher surface area (1420 m<sup>2</sup>/g) and pore volume (0.564 cm<sup>3</sup>/g)</li> <li>▪ XRD patterns for simulated and obtained are similar and present the constituent phases</li> <li>▪ N<sub>2</sub> uptake for ZIF-8 was ~46% higher than that of ZIF-8/CNT</li> </ul>	

11. Ultra sound method



- The resulting ZIF-8 is highly crystalline and has high thermal stability at temperatures below 250 °C [112]

*Continued on next page*

No.	ZIF-8 route	synthesis	XRD pattern	Morphology (SEM)	Outcome	Ref.
12.	Rapid route	synthesis	The XRD data reveal distinct peaks corresponding to crystalline phases, with variations depending on the treatment method. The synthesized sample shows a specific set of diffraction peaks, while subsequent treatments, such as boiling in methanol (MeOH) for 5 and 7 days or in water for 5 days, result in slight changes in peak intensities and positions. This suggests modifications in the crystalline structure, possibly due to solvent-induced transformations, particle growth, or phase changes. The longer boiling duration in methanol seems to produce the most refined or stable crystalline form, as indicated by the sharper peaks in the topmost pattern.	SEM analysis revealed that the particles appear to be spherical and somewhat agglomerated, suggesting possible interparticle interactions or incomplete dispersion. The uniformity of particle size and shape indicates a controlled synthesis process, likely optimized for mono-dispersity.	<ul style="list-style-type: none"> <li>▪ An average particle size of ~85 nm was obtained</li> <li>▪ The crystallite size was calculated to be ~70 nm</li> <li>▪ The synthesized ZIF-8 has a hexagonal facets structure</li> </ul>	[94]

For ZIF-8 to be commercially viable in large-scale carbon capture applications, the development of scalable and cost-effective synthesis methods is critical. While traditional synthesis approaches such as solvothermal, hydrothermal, and mechanochemical routes have demonstrated high purity and tunability, their high solvent usage, long reaction times, and low batch yields hinder industrial scalability.

Several strategies have been explored to enable tonne-scale production of ZIF-8:

1. Solvent-free (mechanochemical) synthesis—This method eliminates organic solvents, significantly reducing production costs and environmental impact. It has been successfully demonstrated for gram-to-kilogram scale production, showing promise for further scale-up.
2. Continuous flow synthesis—Unlike batch methods, continuous flow synthesis offers higher yields, better reproducibility, and reduced reaction times, making it suitable for industrial-scale production.
3. Spray drying and ultrasonic spray pyrolysis (USP)—These approaches enable mass production of uniform ZIF-8 particles with controlled morphology and rapid processing.
4. Green synthesis approaches—The use of water-based synthesis and biomass-derived precursors is being investigated to reduce raw material costs and make ZIF-8 production more sustainable.



The cost of ZIF-8 synthesis remains a key barrier to its widespread deployment in carbon capture technologies. However, the ongoing development of scalable synthesis methods is expected to reduce production costs. Based on current progress, a potential commercialization pathway could involve:

- Short-term (1–3 years): Optimization of continuous flow and mechanochemical synthesis to achieve kilogram-scale production at lower cost.
- Mid-term (3–5 years): Integration of green synthesis approaches and expansion into industrial-scale batch production.
- Long-term (5+ years): Establishment of fully commercial production plants capable of tonne-scale ZIF-8 synthesis, with further reduction in production cost per gram to make it competitive with existing CO<sub>2</sub> adsorbents.

The development of scalable, cost-effective, and environmentally sustainable ZIF-8 synthesis methods remains a key focus area for researchers and industries looking to commercialize MOFs for CO<sub>2</sub> capture.

## 6. CO<sub>2</sub> measurement conditions and techniques

The conditions (temperature, pressure, exhaust gas, and normal gas) of CO<sub>2</sub> play a significant role in CO<sub>2</sub> measuring. The determination of CO<sub>2</sub> levels is influenced by the methods and techniques employed in measurements [23]. Researchers have documented CO<sub>2</sub> measurements under elevated temperatures and pressure conditions [113,114]. Conversely, few researchers have conducted CO<sub>2</sub> measurements under ambient temperature and pressure conditions, including assessments for exhaust and flue gases [100]. Wu et al. [115] measured CO<sub>2</sub> using BELSORP-MAX, Micromeritics Instrument Corp. at 25 °C temperature and up to 1 bar pressure and found that CO<sub>2</sub> measuring capacity of carbon aerogels (20 wt.% ZIF-8 in carbon aerogels) increased by ~2.23 mmol/g. In another study, the CO<sub>2</sub> measurement was carried out using the Wicke-Kallenbach technique at 70–80 °C for 60 min. The maximum selectivity of CO<sub>2</sub> was ~20.29 at 70 °C measuring for 55 min [116]. Martin et al. [117] measured CO<sub>2</sub> at 2 bar pressure and 25–150 °C temperature using chromatography (PerkinElmer, Clarus 400) equipped with a TCD detector and found that the selectivity of H<sub>2</sub>/CO<sub>2</sub> gas mixture (ZIF-8 membrane) was ~7.8 at 100 °C and 2 bar pressure. The CO<sub>2</sub> adsorption measured at ambient pressure and the room temperature was carried out using Pyris Diamond TG/DTA Perkin Elmer Analysis, and CO<sub>2</sub> uptake was ~0.4 mmol/g for the ZIF-8 membrane [118]. Similarly, Ding et al. [119] measured CO<sub>2</sub> uptake using the volumetric determination method at ambient temperature and pressure and found that CO<sub>2</sub> uptake of ZIF-L was ~1.56 mmol/g. In another report, the CO<sub>2</sub> uptake was ~0.94 mmol/g [110]. However, in another study, the measurement of CO<sub>2</sub> from flue gas was carried out using gas chromatography (GC) equipped with thermal conductivity detectors (TCDs) (Agilent Technologies, Palo Alto, CA). The permeance and selectivity of CO<sub>2</sub> (flue gases) on polymer/zeolite Y (ZY) (Pebax/PEG-DME500 25/75) composite membranes were ~661 GPU and 30 [120]. Table 7 summarizes the CO<sub>2</sub> measuring methods with the condition.

**Table 7.** Details of CO<sub>2</sub> measuring techniques (instruments) with measuring conditions (temperature and pressure).

No.	CO <sub>2</sub> measuring instrument (technique)	Composite/membrane	Pressure	Temperature (°C)	CO <sub>2</sub> uptake/permeability	Ref.
1.	Gravimetric analysis (IGA-001)	ZIF-8/zeolite-13X	0–1000 mbar	25	1.8/4.1 mmol/g	[121]
2.	Monometric technique	ZIF-8 (16 wt.%) modified polysulfone	1.3 bar	25, 50, and 65	8/9.5/10.5	[122]
3.	Constant pressure variable volume method	PIM-1/ZIF-8 MMMs	4 bar	Room temperature	9.88	[18]
4.	Micromeritics TriStar II 3020	ZIF-8 on bacterial cellulose	1 bar	Room temperature	0.15 (BC) and 1.63 ZIF-9@BC)	[123]
5.	Gas chromatography (Alicat Scientific, MC-100CCM-D)	PBI-based MMMs with ZIF-8 (10–20 wt.%)	3–6 bar	Room temperature	65 cm <sup>3</sup> /min	[14]
7.	Drum-type gasmeter (TG Series, Ritter Apparatebau GmbH)	Ceramic zeolite membrane (H-ZSM-5)	9 bar	300	62 × 10 <sup>-7</sup> mol/s/m <sup>2</sup> Pa.	[124]
8.	Constant pressure variable volume method	Core-shell mesoporous 5A@silica (5A@MS)	1 bar	Room temperature	3.41	[125]

## 7. Factors affecting the capture/adsorption of CO<sub>2</sub> by ZIF-8

### 7.1. Synthesis method

The synthesis method used to produce ZIF-8 can have a significant impact on its properties, including its performance in CO<sub>2</sub> capture applications. The synthesis method affects the particle size, crystallinity, surface area, and other structural features of ZIF-8, which in turn influence its ability to adsorb CO<sub>2</sub> [129]. Here are some key considerations regarding the effect of synthesis methods on CO<sub>2</sub> capture by ZIF-8:

#### 7.1.1. Particle size

The particle size of synthesized ZIFs/ZIF-8 in CO<sub>2</sub> capturing plays an important role, as the particle size of ZIFs reduces the performance of the filter membrane increases [127]. It has been reported that incorporation of ZIF-8 (45 nm) as filler in polybenzimidazole (PBI) based MMMs increased the membrane performance ~ by 46% [128]. Chen et al. [108] reported that the incorporation of 20 wt.% of ZIF-8 (50 nm) in PBI-based MMMs increased the H<sub>2</sub> approximately six times, and the H<sub>2</sub>/CO<sub>2</sub> selectivity increased nearly by 55% compared to the bare PBI polymer membrane [129]. The permeability and selectivity of CO<sub>2</sub>/CH<sub>4</sub> depend on the dispersion of ZIF-8 crystal in MMMs. It was demonstrated that the incorporation of 5 wt.% ZIF-8 (45–450 nm) in the polymer of intrinsic microporosity (PIM) (to form MMMs) enhanced the permeability and selectivity of CO<sub>2</sub> by approximately 43% and ~6.4%, respectively, for ZIF-8 (120 nm) due to homogeneous dispersion [130]. Table 8 summarizes the effect of particle size of ZIF-8 on the permeability and selectivity of CO<sub>2</sub>.

**Table 8.** The effect of particle size of ZIF-8 on permeability and selectivity of CO<sub>2</sub> [131].

No.	Membrane	Weight ratio (PIM-1:ZIF-8)	Permeability (barrier)				Ideal selectivity	
			Before aging		After aging (40 days)		Before aging	After aging (40 days)
			CO <sub>2</sub>	CH <sub>4</sub>	CO <sub>2</sub>	CH <sub>4</sub>	CO <sub>2</sub> /CH <sub>4</sub>	CO <sub>2</sub> /CH <sub>4</sub>
1.	PIM-1	1:0	9336	1453	6343	895	6.43	7.08
2.	PIM-1/ZIF-8A*	1:0.05	6846	2709	4292	1527	2.53	2.81
3.	PIM-1/ZIF-8B*	1:0.05	9667	852	3923	283	11.35	13.85
4.	PIM-1/ZIF-8C*	1:0.05	7018	1357	5933	988	5.17	6.01
5.	PIM-1/ZIF-8D*	1:0.05	6737	752	5255	532	8.95	9.88
6.	PIM-1/ZIF-8	1:0.1	4815	320	NA	NA	105.00	NA
7.	PIM-1/ZIF-8	1:0.16	4270	230	NA	NA	18.60	NA
8.	PIM-1/ZIF-8	1:0.32	6820	510	NA	NA	13.40	NA
9.	PIM-1/ZIF-8	1:0.48	6300	430	NA	NA	14.70	NA

\*Note: ZIF-8A, ZIF-8B, ZIF-8C, and ZIF-8D denote the particle size of ZIF-8, which starts from 45, 120, 250, and 45 nm, respectively.

Overall, it has been concluded that the particle size of ZIF-8 plays a significant role in membrane performance. However, a few results suggested that dispersion of ZIF-8 particles in MMMs can alter the results, i.e., proper dispersion of ZIF-8 can improve the permeability as well as selectivity of CO<sub>2</sub>.

#### 7.1.2. Structure and surface area

The ZIF-8 structure is highly effective for CO<sub>2</sub> capturing [132]. The strong chemical affinity of the zinc and imidazolate groups in the ZIF-8 structure for CO<sub>2</sub> also contributed to the high efficiency of CO<sub>2</sub> capture [133]. The unique structure of ZIF-8, which consists of zinc ions and organic linkers arranged in a tetrahedral arrangement (Figure 11) [134], enables a large surface area [135]. This enables a high affinity for CO<sub>2</sub> molecules, which can be easily adsorbed onto the surface of the MOF. One of the key benefits of using ZIF-8 for CO<sub>2</sub> capture is its high selectivity for CO<sub>2</sub> unlike other MOFs, which may also adsorb other gases such as nitrogen or methane; ZIF-8 has been shown to have a strong preference for CO<sub>2</sub> [136]. This means that it is more effective at separating CO<sub>2</sub> from other gases in the atmosphere, enabling more efficient capture and storage. Another advantage of ZIF-8 is its stability in harsh conditions. Unlike other MOFs, which can lose their porosity and surface area over time, ZIF-8 has been shown to maintain its structure even under high temperatures and pressures [137]. This means that it can be used in a wide range of applications, from capturing CO<sub>2</sub> from flue gases to purifying air in enclosed spaces; the unique structure of ZIF-8 has a significant impact on its ability to effectively capture CO<sub>2</sub>. Its high porosity and selectivity for CO<sub>2</sub> make it a promising candidate for use in CO<sub>2</sub> capture and storage technologies.

Yuel et al. [136] reported that normal ZIFs (without modification) may have certain limitations, low solubility of metal salts, and formation of unwanted topologies. To overcome such a challenging issue, solvent-assisted ligands/linker exchange (SALE) has been used. This is a post-synthesis modification on the structure of ZIFs where the organic linker is exchanged with another suitable solvent medium. This structural modification increases the CO<sub>2</sub> adsorption capacity of ZIFs. The CO<sub>2</sub>

uptake of NO<sub>2</sub> and SALE modified increases by approximately 32% and 100%. However, after 120 h of SALE modification, the CO<sub>2</sub> uptake is 4.23 mmol/g [136].

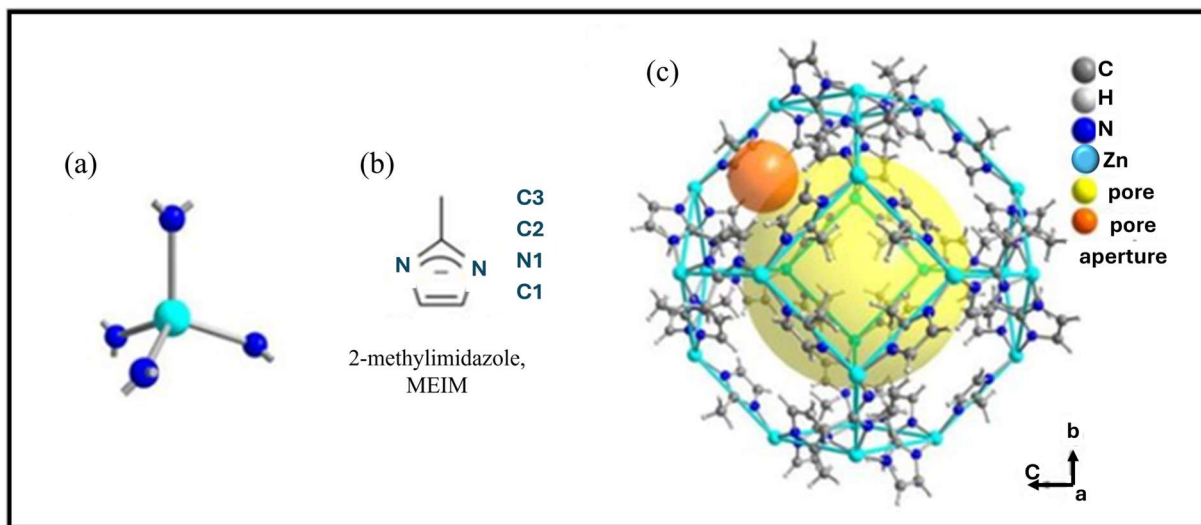


**Figure 11.** ZIF-8 (a, b) building blocks and (c) unit structure (Reproduced from Ref. [134] with permission).

In another study, it has been demonstrated that the shape (cavity) of fabricated ZIFs can enhance the CO<sub>2</sub> uptake. Chen et al. [108] reported that two-dimensional ZIF with a cushion-shaped cavity (leaf-like crystal structure) demonstrates approximately 54% higher CO<sub>2</sub> adsorption than ZIF-8 nanocrystalline due to smaller pore size and high density of ZIF-L than ZIF-8. Table 9 summarizes the CO<sub>2</sub> uptake and specific surface area obtained from previous reports. In view of the above results, it can be concluded that the structural modification in ZIFs increases the CO<sub>2</sub> uptake.

**Table 9.** The CO<sub>2</sub> uptake and specific surface area.

No.	Sample	Structure	Temperature (K)	Pressure (MPa)	S <sub>BET</sub> (m <sup>2</sup> g <sup>-1</sup> )	CO <sub>2</sub> uptake (mmol g <sup>-1</sup> )	Ref.
1.	Hierarchical structures (hydrothermal treated)	ZIF-L Leaf-like	298	0.1	304	1.56	[119]
2.	Two-dimensional leaves	ZIF-L Leaf-like	298	0.1	161	0.94	[108]
3.	ZIF-8 nanocrystalline	-	298	0.1	1450	0.68	[139]
4.	Nanostructured ZIF-8	SALE modified	298	0.1	-	1.62	[136]
5.	Nanostructured ZIF-8	NO <sub>2</sub> modified	298	0.1	-	1.02	[136]

### 7.1.3. Effect of porosity

The porosity of ZIF-8 is a critical factor that can be controlled and optimized during the synthesis process and it significantly influences its performance in CO<sub>2</sub> capture. There are some effects of porosity as a synthesis parameter for ZIF-8 in the context of CO<sub>2</sub> capture [23]. Notably, zeolitic-type porous

materials have gained attention for their advanced technological and industrial applications [139]. Among these, MOFs, a type of hybrid material, have been a subject of considerable effort, with their application spanning various industrial uses, including separation, catalysis, and sensing [140]. A specific example is the attention given to ZIFs in the context of CO<sub>2</sub> adsorption. The porosity of ZIFs plays a crucial role in this process, as illustrated in Figure 12 [141], where the impact of porosity on membrane support is depicted. Studies indicate that ZIFs with larger pore sizes exhibit favorable interactions in CO<sub>2</sub> capture [125]. Additionally, effective CO<sub>2</sub> adsorption requires adsorbents with significant volume and surface areas of pores. It is essential that these adsorbents exhibit fundamental properties such as high mechanical, thermal, and chemical stability, low heat capacity, high adsorption capacity, and cost-effectiveness [129].

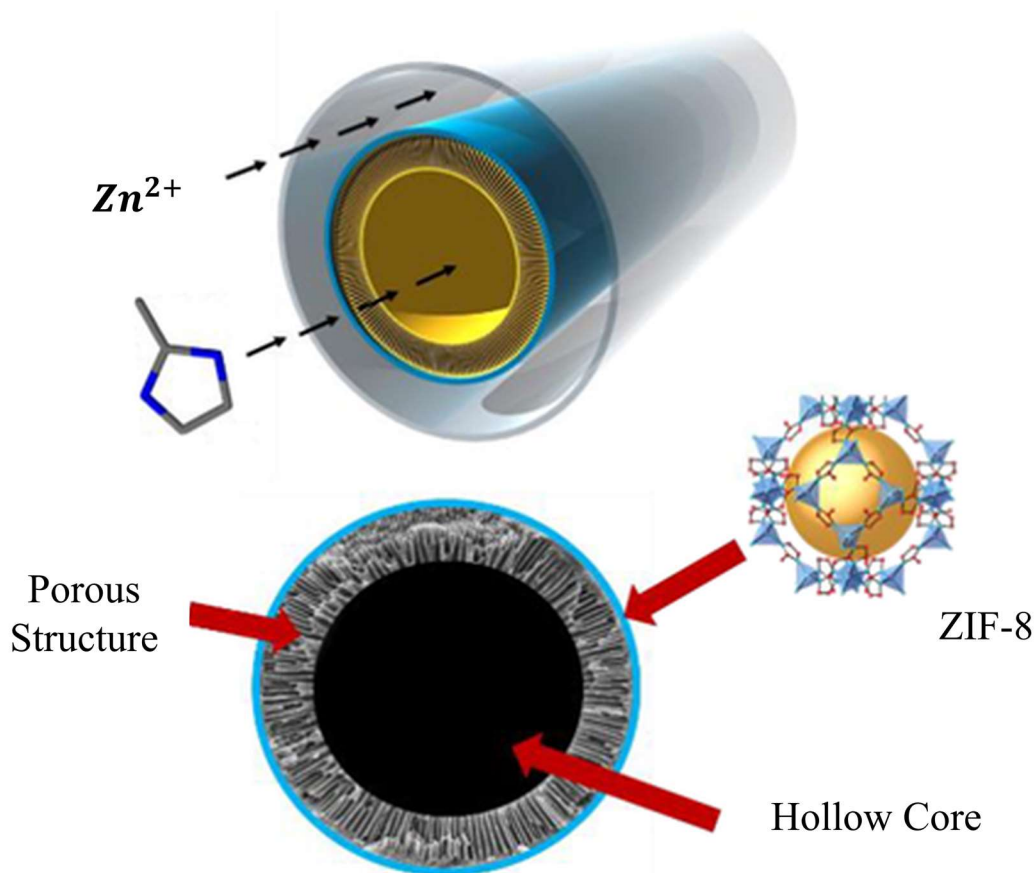


**Figure 12.** Processing of a supported ZIF-8 hollow fiber membrane, and a cross-section diagram showing the hollow core, porous Torlon structure, and ZIF-8 on the surface of the support (Reproduced from Ref. [141] with permission).

#### 7.1.4. Cost and scalability

The choice of synthesis method can also impact the cost and scalability of ZIF-8 production. Some methods such as the stoichiometric molar ratios of zinc ions and 2-methylimidazole precursor and rapid synthesis routes are more cost-effective and suitable for large-scale production [94,142].

The reproducibility of the synthesis method is crucial for the consistent production of ZIF-8 with desired properties. Moreover, variability in synthesis conditions may lead to variations in material performance [143].

Researchers explore various synthesis routes, including solvothermal, microwave-assisted, hydrothermal, and room-temperature methods, to tailor the properties of ZIF-8 for optimal CO<sub>2</sub> capture. The choice of synthesis method depends on the specific requirements of the application and the desired characteristics of the material [144]. Optimization of synthesis conditions is an ongoing area of research to improve the efficiency of ZIF-8 for CO<sub>2</sub> capture.

## 7.2. Metal linker and ligands

The CO<sub>2</sub> capture performance by MOFs, particularly the ZIF-8 depends on the choice of metal linker and ligands. Here are some considerations for the effect of metal linkers and ligands on CO<sub>2</sub> capture in ZIF-8.

### 7.2.1. Metal linker

The metal ion in the linker plays a crucial role. Different metal ions have different affinities for CO<sub>2</sub>. Zinc is commonly used in ZIF-8, and its coordination properties influence the adsorption capacity and selectivity for CO<sub>2</sub> [145]. Other metal ions with different Lewis acidities may alter the interaction between the framework and CO<sub>2</sub> molecules.

In addition, the coordination environment around the metal ion can influence the structural stability of ZIF-8 and its ability to adsorb CO<sub>2</sub>. It can also affect the energy of interaction between the metal ion and CO<sub>2</sub>.

### 7.2.2. Ligands

The organic ligands in ZIF-8 contain nitrogen-containing imidazolate groups. The presence of specific functional groups, such as amino or alkyl amino groups, in the ligands can enhance the interaction with CO<sub>2</sub> through hydrogen bonding or other interactions, thereby improving the capture efficiency [97]. The choice of ligands can influence the size of the pores in the MOF. Tuning the pore size is crucial for optimizing the adsorption capacity and selectivity for CO<sub>2</sub>. Larger or smaller pores may be more suitable for different CO<sub>2</sub> capture applications [136]. It has been reported that functional ligands with specific properties, such as open metal sites or polar functional groups, can enhance the interaction with CO<sub>2</sub> and improve the overall performance of ZIF-8 for carbon capture [146].

The combination of specific metal ions and ligands can result in synergistic effects that enhance CO<sub>2</sub> capture properties. Optimizing the pairing of metal ions and ligands can lead to MOFs with improved performance.

## 7.3. Impurities in a gas stream

The presence of gas impurities in the feed gas stream can have various effects on the performance of ZIF-8 for CO<sub>2</sub> capture. Impurities may interact with ZIF-8, affecting its adsorption capacity, selectivity, and overall efficiency [147]. Here are some considerations regarding the effects of gas impurities on CO<sub>2</sub> capture by ZIF-8: Flue gas comprises not only CO<sub>2</sub> and N<sub>2</sub> but also significant impurities like H<sub>2</sub>O, O<sub>2</sub>, and SO<sub>2</sub>, negatively impacting traditional amine-based CO<sub>2</sub> scrubbing [148].

Research on CO<sub>2</sub> capture from flue gas using ZIFs has predominantly encompassed pure CO<sub>2</sub> adsorption or its capture from CO<sub>2</sub>/N<sub>2</sub> mixtures [148,149].

### 7.3.1. Interactions with functional groups

Gas impurities may interact with the functional groups present in ZIF-8's structure. These interactions can influence the adsorption behavior and stability of the material, potentially leading to changes in its performance [150].

### 7.3.2. Humidity effects

Moisture in the gas stream can also be considered an impurity. ZIF-8 and other MOFs can be sensitive to water, potentially leading to structural changes or decreased adsorption capacity [151]. The adsorption capacity of CO<sub>2</sub> for activated carbon (AC) based ZIF-8 (AC@ZIF-8) decreased by ~16.27% while relative humidity increased by ~61% [152]. To address the challenges posed by gas impurities, researchers often conduct comprehensive studies to understand the interaction mechanisms and develop strategies to enhance the robustness of ZIF-8.

## 8. CO<sub>2</sub> absorption by various ZIF filter/composite systems

The membrane's filter materials and the design of the filter play an important role in the capture of CO<sub>2</sub>. Generally, nanoporous ZIF-8 can be used to prepare the polymer membrane, which enhances the performance of the membrane [153]. In addition, various substrates such as copper net, titanium support tubular  $\alpha$ -alumina support, Zn-related nanofibers, and Nylon membrane were used with ZIFs/ZIF-8 for CO<sub>2</sub> capture. It has been reported that the ZIF-8 membrane was prepared on alumina hollow fiber alumina porous support, and the various membrane filters were prepared for CO<sub>2</sub> capturing using ZIF-8. The uptake of CO<sub>2</sub> by various filter/composite systems are summarized in Table 10.

**Table 10.** CO<sub>2</sub> uptake by various filter/composite systems.

No.	Absorbent	S <sub>BET</sub> (m <sup>2</sup> /g)	Conc. of CO <sub>2</sub>	Temperature (°C)	CO <sub>2</sub> uptake (mmol/g)	Ref.
1.	ZIF-8	1579	1 atm	25	0.88	[104]
2.	ZDC-850	1873	1 atm	25	3.50	[104]
3.	ZIF-8/PAN	1178	1 atm	25	4.20	[104]
4.	ZDC-850/PAN	1046	1 atm	25	3.38	[104]
5.	ZIF-8	1016	1 bar	25	0.60	[154]
6.	ZIF-PAN	888	1 bar	25	0.28	[154]
7.	ZIF-8-8s	283	1 bar	20	1.44	[123]
8.	ZIF-8	1169	1 bar	0	1.41	[155]
9.	NH <sub>2</sub> -ZIF-8	886	1 bar	0	2.12	[156]
10.	ZIF-100	595	1 atm	0	1.3	[127]
				25	0.6	

In the past few decades, ZIFs have been given attention due to their high porosity and chemical and thermal stabilities. Various ZIFs are developed as membrane filter material as well as composites for CO<sub>2</sub> capture [113]. It has been reported that various polymeric membranes have been modified with ZIFs to prepare MMMs [114]. It has been demonstrated that the permeability of CO<sub>2</sub> and H<sub>2</sub> can be improved with the addition of ZIFs in membrane/composite [99]. Moreover, the incorporation of 15 wt.% ZIF-90 in 6FDA-DFM increases the permeability of CO<sub>2</sub> ~45% compared to pure 6FDA-DFM [157]. In another study, it was reported that pure NH<sub>2</sub>-MIL-53(Al) demonstrates ~34% CO<sub>2</sub> selectivity while incorporating 25 wt.% PSF increases the CO<sub>2</sub> selectivity ~56% [158]. Table 11 summarizes various ZIF based-membranes/composites for CO<sub>2</sub> capture.

**Table 11.** Various ZIF-based membranes/composites for CO<sub>2</sub> capture.

No.	Membrane/composite	CO <sub>2</sub> uptake/permeability	CO <sub>2</sub> selectivity	Ref.
1.	15 wt.% ZIF-90@DFM	46%	-	[159]
2.	Zn/Co-ZIF (10 wt.%)/6FDA-ODA Zn/Co-ZIF (7.5 wt.%)/6FDA-ODA	104% 41%	-	[158]
3.	5A@mesoporous silica 5A@MSA-30 wt. %	83 %	--	[157]
4.	Na-ZSM-5 B-ZSM-5 (MFI type zeolitic membrane)	84% 67%	-	[157]
5.	ZIF-8 modified with benzotriazole	27%	-	[160]
6.	ZIF-8/polymethylphenylsiloxane (PMPS) MMMs	63%	-	[161]
7.	ZIF-8/PBI (20 wt.% ZIF-8)		24.7	[162]
8.	PSf/ZIF-8 (polysulfone) MMMs	67%	-	[163]
9.	ZIF-8 and polybenzimidazole (PBI)	55%	-	[164]
10.	30 wt.% ZIF-8@PBI	-	26.8	[122]
11.	25 wt.% ZIF-8@polyimide-amide polymer	-	52.5	[141]
12.	20 vol.% ZIF-8@PIM	-	18.3 ± 1.9	[165]

Overall, it can be concluded that incorporating ZIFs in MMMs/composites increases the selectivity/permeability of CO<sub>2</sub>. Among the ZIFs, ZIF-8 has good CO<sub>2</sub> uptake to other prepared ZIFs.

ZIF-8-based materials have demonstrated promising CO<sub>2</sub> adsorption properties in laboratory environments; however, their performance in real-world flue gas conditions remains a critical factor for industrial deployment. Flue gas streams typically contain CO<sub>2</sub> (10%–15%), N<sub>2</sub>, H<sub>2</sub>O vapor, O<sub>2</sub>, NO<sub>x</sub>, SO<sub>2</sub>, and other trace contaminants that influence adsorption selectivity, stability, and regeneration efficiency. ZIF-8 exhibits moderate CO<sub>2</sub> uptake (0.88–1.62 mmol/g at ambient conditions), making it suitable for low-to-moderate CO<sub>2</sub> concentrations in flue gas. Its hydrophobic nature provides relative stability in humid environments, but modifications such as amine-functionalization and hybrid composites enhance CO<sub>2</sub> selectivity and adsorption performance in competitive gas conditions. Additionally, when integrated into mixed-matrix membranes, ZIF-8 has been shown to improve CO<sub>2</sub>/N<sub>2</sub> selectivity, reducing energy losses in gas separation processes.

Long-term stability is another key aspect of practical deployment. While pure ZIF-8 remains stable under moderate operating conditions, it may degrade under prolonged exposure to high temperatures (>550 °C) and acidic gases such as SO<sub>2</sub> and NO<sub>x</sub>. However, composite formulations



incorporating polymers or hybrid MOFs have demonstrated enhanced thermal, chemical, and hydrolytic stability, enabling sustained adsorption-desorption cycles. Studies indicate that ZIF-8 can maintain stable CO<sub>2</sub> uptake over 50+ adsorption-desorption cycles, making it a promising material for pressure swing adsorption (PSA) and temperature swing adsorption (TSA) processes.

A major advantage of ZIF-8 is its low regeneration energy compared to traditional amine-based solvents, requiring significantly lower energy for desorption (~50 kJ/mol CO<sub>2</sub> versus ~140 kJ/mol CO<sub>2</sub> for amines). Its low heat of adsorption makes it suitable for vacuum and mild temperature swing adsorption processes, reducing the overall energy footprint of CO<sub>2</sub> capture operations. Recent advances in ZIF-8 hybrid materials have optimized CO<sub>2</sub> affinity while maintaining low regeneration costs, improving the economic feasibility of industrial-scale carbon capture. Despite these advantages, challenges remain, particularly in terms of competitive adsorption with H<sub>2</sub>O and other flue gas components, which can reduce CO<sub>2</sub> uptake efficiency. Hydrophobic surface modifications and functional group tuning are active research areas to mitigate this issue. Furthermore, large-scale synthesis of ZIF-8 remains a challenge, requiring cost-effective production strategies for broader industrial adoption. Future research should consist of hybridizing ZIF-8 with other MOFs or adsorbents to enhance selectivity, stability, and long-term performance in flue gas conditions, ensuring its viability as an efficient and scalable CO<sub>2</sub> capture material.

## 9. Advantages of ZIF-8 for CO<sub>2</sub> capture

ZIF-8 is a highly porous, thermally, and chemically stable material with a large surface area and pore volume, which is best suitable for the preparation of membrane/composite material for CO<sub>2</sub> capture. It has been reported that the permeability of H<sub>2</sub> on ZIF-8 grown hollow ceramic tube is ~ 67% [106]. In another study, it was reported that the permeabilities of H<sub>2</sub> and CO<sub>2</sub> on the ZIF-8/rGO (graphene oxide) membrane are ~ 68% and 65%, respectively [24]. In another study, it was reported that the CO<sub>2</sub> capture capacities of ZTF-1, MGMOF-74, ZIF-177, and ZIF-67 are ~5.4, 4.3, 6.2, 8.3, respectively [166,167]. It has been demonstrated that ZIF-8 can increase the selectivity and permeability of gas separation [168]. Therefore, ZIF-8 can be used as membrane material for the development of a filter to absorb the CO<sub>2</sub>. In view of the above, the advantages of ZIF-8 over other developed materials (for CO<sub>2</sub> capture) are listed as follows [169]:

- ZIF-8 has a high affinity for CO<sub>2</sub>, making it highly efficient at capturing and retaining the gas.
- Its porous structure enables large amounts of CO<sub>2</sub> to be captured within a small volume, making it a space-efficient option for CO<sub>2</sub> capture.
- ZIF-8 is stable and robust, making it suitable for use in various conditions and environments.
- The material can be easily regenerated for reuse, enabling a more sustainable and cost-effective approach to CO<sub>2</sub> capture.
- ZIF-8 is relatively low-cost compared to other materials used for CO<sub>2</sub> capture, making it an affordable option for large-scale applications.
- The material has a high surface area, enabling more efficient CO<sub>2</sub> absorption and increasing its overall effectiveness.
- ZIF-8 has a high selectivity for CO<sub>2</sub>, meaning it effectively captures the gas while minimizing the capture of other gases or impurities.
- The material can be synthesized in a controlled manner, enabling the production of high-quality, consistent batches of ZIF-8 for use in CO<sub>2</sub> capture applications.

The practical processability of ZIFs remains a critical challenge in their large-scale application for CO<sub>2</sub> capture, as their powder form limits direct industrial use. One of the most promising approaches to improve processability is the integration of ZIFs into polymers, leading to the development of three-dimensional (3D) sorbents such as membranes and aerogels. ZIF-8-based MMMs have gained attention due to their enhanced gas separation performance, where the incorporation of ZIF-8 into polymeric matrices improves selectivity, permeability, and mechanical strength [170]. Similarly, ZIF-8 aerogels, with their high porosity and ultra-lightweight structure, have demonstrated superior CO<sub>2</sub> adsorption capacity and rapid diffusion kinetics, making them suitable for direct air capture and industrial gas separation applications [123]. However, challenges such as heterogeneous dispersion, polymer-ZIF interfacial adhesion issues, and long-term stability under industrial conditions remain critical barriers to their commercialization. Advancements in polymer functionalization, ligand modification, and hybrid aerogel structures have been explored to address these limitations, paving the way for more efficient and scalable ZIF-8-based CO<sub>2</sub> capture systems [170].

While ZIF-8 is widely recognized for its exceptional structural properties and gas separation efficiency, its biocompatibility and cytotoxicity are also important considerations, particularly for applications where environmental and biological exposure is relevant. In the context of ZIFs, cytotoxicity refers to how these materials interact with living cells—whether they are toxic to human or environmental cells when inhaled, ingested, or exposed to biological systems. This toxicity is often linked to zinc ion (Zn<sup>2+</sup>) release, oxidative stress, or cellular uptake of nanoparticles. The biocompatibility and cytotoxicity of ZIFs are key considerations for their industrial, biomedical, and environmental applications.

ZIF-8, the most extensively studied ZIF, is generally regarded as biocompatible under moderate exposure levels, exhibiting low inherent toxicity due to its chemical stability and minimal interaction with biological systems [170]. However, potential cytotoxicity concerns arise from zinc ion release, which can occur under acidic or highly reactive environments, leading to cellular stress and oxidative effects. Studies indicate that ZIF-8 degradation in biological fluids can influence its toxicity profile, with prolonged exposure or high concentrations potentially impacting cell viability.

Structural modifications, such as surface functionalization and polymer coatings, have been explored to enhance biocompatibility by preventing excessive ion leaching and improving stability [170]. In environmental applications, ZIFs are considered to have low ecotoxicity, and their controlled degradation pathways make them suitable for long-term use in gas separation and adsorption technologies. The continued development of engineered ZIF-based materials focuses on balancing structural integrity, controlled degradation, and minimal biological impact, ensuring their safe and effective integration into practical applications.

ZIF-8, like most MOFs, is typically synthesized as a fine crystalline powder, which is highly porous but difficult to handle in adsorption-based processes. For practical CO<sub>2</sub> capture applications, ZIF-8 needs to be shaped into structurally stable forms that maintain high adsorption capacity while ensuring mechanical durability and efficient gas transport. Various shaping techniques have been explored to transform ZIF-8 powders into pellets, granules, monoliths, and composite structures, each offering distinct advantages and challenges. Pelletization is a commonly used method, where ZIF-8 powders are compressed with binders or additives to form mechanically stable adsorbents, though excessive binder content can reduce porosity and adsorption efficiency. Monolithic structures, synthesized through direct templating or additive manufacturing, provide improved gas diffusion properties and reduce pressure drop in adsorption columns, making them suitable for PSA, TSA, and

vacuum swing adsorption (VSA) processes. Bead-based ZIF-8 composites, formed via spray-drying or gelation techniques, offer enhanced handling properties and can be optimized for cyclic adsorption-desorption performance. The shaping process must balance mechanical strength, gas diffusion, and adsorption efficiency to ensure that ZIF-8-based materials perform optimally under industrial CO<sub>2</sub> separation conditions. By optimizing shaping processes, ZIF-8 can be effectively adapted for industrial-scale adsorption, offering an alternative to traditional sorbents in PSA, TSA, and TVSA-based CO<sub>2</sub> separation systems. Researchers have focused on binder-free shaping techniques, hybrid MOF-polymer composites, and 3D-printed MOF architectures to achieve scalable, structurally stable, and high-performance CO<sub>2</sub> adsorbents.

## 10. Conclusions and future scope

In conclusion, we delved into the synthesis methods/routes employed for creating ZIF-8, specifically for CO<sub>2</sub> capture applications. We encompassed an overview of various synthesis techniques and their corresponding characterization results, elucidating the impacts of particle size, porosity, and structural attributes on CO<sub>2</sub> capture efficiency. Furthermore, the investigation extended to the utilization of materials/composites for enhancing CO<sub>2</sub> adsorption, along with a comprehensive discussion on the diverse techniques/equipment utilized for precise CO<sub>2</sub> measurement.

A critical focus was placed on the distinct advantages of ZIF-8 over alternative materials for CO<sub>2</sub> capture. Despite its immense potential, the challenge of achieving reproducibility in most fabrication methods remains significant. Addressing this issue is pivotal to ensuring consistent performance, and the exploration of a rapid synthesis route emerged as a standout option due to its efficiency in terms of production rate, time, and cost-effectiveness of precursors. While membranes for CO<sub>2</sub> capture have demonstrated promise, their predominance at the lab scale necessitates further research to facilitate a transition to industrial implementation.

In summary, the potential of ZIF-8 and its composites for CO<sub>2</sub> capture is undeniable, positioning them as emerging materials of great significance. For eventual commercialization, continued refinement in fabrication techniques is imperative. Among these techniques, the rapid synthesis route is particularly promising, showcasing efficiency in producing ZIF-8 materials with remarkable CO<sub>2</sub> capture capabilities. This avenue holds the key to transforming these materials from a realm of potential into a practical reality, offering a sustainable solution for addressing the pressing challenges of CO<sub>2</sub> capture and contributing to a greener future.

## Use of AI tools declaration

The authors declare they have not used Artificial Intelligence (AI) tools in the creation of this article.

## Acknowledgments

This project has received funding from the European Union's Horizon 2020 research and innovation Programme under the Marie Skłodowska-Curie Grant Agreement No 847639, PASIFIC Postdoctoral Fellowship Programme. The content of this article does not reflect the official opinion of the European Union. Responsibility for the information and views expressed herein lies entirely with the author(s).

## Author contributions

Conceptualization: A.V.; methodology: A.V., A.S. (Aman Singh) and A.S. (Angaraj Singh); software: A.V.; validation: A.S. (Aman Singh), K.K. and A.V.; formal analysis: A.V., A.S. (Aman Singh) and A.S. (Angaraj Singh); investigation: A.V., A.S. (Aman Singh) and A.S. (Angaraj Singh); resources: A.V. and M.W.; data curation: A.V., A.S. (Aman Singh) and K.K.; writing—original draft preparation: A.V., A.S. (Aman Singh), A.S. (Angaraj Singh) and K.K.; writing—review and editing: K.K., M.W. and A.V.; visualization: A.V.; supervision: A.V. and M.W.; project administration: A.V. and M.W.; funding acquisition: A.V. and M.W. All authors have read and agreed to the published version of the manuscript.

## Conflict of interest

The authors declare no conflict of interest.

## References

1. Keshavarz L, Ghaani MR, MacElroy JMD, et al. (2021) A comprehensive review on the application of aerogels in CO<sub>2</sub>-adsorption: Materials and characterisation. *Chem Eng J* 412: 128604. <https://doi.org/10.1016/j.cej.2021.128604>
2. Rybak A, Rybak A, Boncel S, et al. (2022) Hybrid organic-inorganic membranes based on sulfonated poly (ether ether ketone) matrix and iron-encapsulated carbon nanotubes and their application in CO<sub>2</sub> separation. *RSC Adv* 12: 13367–13380. <https://doi.org/10.1039/d2ra01585d>
3. Sun Z, Dong J, Chen C, et al. (2021) Photocatalytic and electrocatalytic CO<sub>2</sub> conversion: From fundamental principles to design of catalysts. *J Chem Technol Biotechnol* 96: 1161–1175. <https://doi.org/10.1002/jctb.6653>
4. Goda MN, Abdelhamid HN, Said AEAA (2020) Zirconium oxide sulfate-carbon (ZrOSO<sub>4</sub>@C) derived from carbonized UiO-66 for selective production of dimethyl ether. *ACS Appl Mater Interfaces* 12: 646–653. <https://doi.org/10.1021/acsami.9b17520>
5. Takht Ravanchi M, Sahebdehfar S (2021) Catalytic conversions of CO<sub>2</sub> to help mitigate climate change: Recent process developments. *Process Saf Environ Prot* 145: 172–194. <https://doi.org/10.1016/j.psep.2020.08.003>
6. Abdelhamid HN, Mathew AP (2022) Cellulose-based nanomaterials advance biomedicine: A review. *Int J Mol Sci* 23: 5405. <https://doi.org/10.3390/ijms23105405>
7. Younas M, Rezakazemi M, Daud M, et al. (2020) Recent progress and remaining challenges in post-combustion CO<sub>2</sub> capture using metal-organic frameworks (MOFs). *Prog Energy Combust Sci* 80: 100849. <https://doi.org/10.1016/j.pecs.2020.100849>
8. Kayal S, Sun B, Chakraborty A (2015) Study of metal-organic framework MIL-101(Cr) for natural gas (methane) storage and compare with other MOFs (metal-organic frameworks). *Energy* 91: 772–781. <https://doi.org/10.1016/j.energy.2015.08.096>
9. Qin JS, Yuan S, Alsalmeh A, et al. (2017) Flexible zirconium MOF as the crystalline sponge for coordinative alignment of dicarboxylates. *ACS Appl Mater Interfaces* 9: 33408–33412. <https://doi.org/10.1021/acsami.6b16264>

10. Joharian M, Morsali A (2019) Ultrasound-assisted synthesis of two new fluorinated metal-organic frameworks (F-MOFs) with the high surface area to improve the catalytic activity. *J Solid State Chem* 270: 135–146. <https://doi.org/10.1016/j.jssc.2018.10.046>
11. Bux H, Liang F, Li Y, et al. (2009) Zeolitic imidazolate framework membrane with molecular sieving properties by microwave-assisted solvothermal synthesis. *J Am Chem Soc* 131: 16000–16001. <https://doi.org/10.1021/ja907359t>
12. Park KS, Ni Z, Côté AP, et al. (2006) Exceptional chemical and thermal stability of zeolitic imidazolate frameworks. *Proc Natl Acad Sci USA* 103: 10186–10191. <https://doi.org/10.1073/pnas.0602439103>
13. Sorribas S, Zornoza B, Teílez C, et al. (2012) Ordered mesoporous silica-(ZIF-8) core-shell spheres. *Chem Commun* 48: 9388–9390. <https://doi.org/10.1039/C2CC34893D>
14. Sánchez-Láinez J, Zornoza B, Friebe S, et al. (2016) Influence of ZIF-8 particle size in the performance of polybenzimidazole mixed matrix membranes for pre-combustion CO<sub>2</sub> capture and its validation through interlaboratory test. *J Membr Sci* 515: 45–53. <https://doi.org/10.1016/j.memsci.2016.05.039>
15. Kim D, Kim W, Buyukcakir O, et al. (2017) Highly hydrophobic ZIF-8/carbon nitride foam with hierarchical porosity for oil capture and chemical fixation of CO<sub>2</sub>. *Adv Funct Mater* 27: 1700706. <https://doi.org/10.1002/adfm.201700706>
16. Gong X, Wang Y, Kuang T (2017) ZIF-8-based membranes for carbon dioxide capture and separation. *ACS Sustain Chem Eng* 5: 11204–11214. <https://doi.org/10.1021/acssuschemeng.7b03613>
17. Zhang Z, Xian S, Xi H, et al. (2011) Improvement of CO<sub>2</sub> adsorption on ZIF-8 crystals modified by enhancing basicity of surface. *Chem Eng Sci* 66: 4878–4888. <https://doi.org/10.1016/j.ces.2011.06.051>
18. Yahia M, Phan Le QN, Ismail N, et al. (2021) Effect of incorporating different ZIF-8 crystal sizes in the polymer of intrinsic microporosity, PIM-1, for CO<sub>2</sub>/CH<sub>4</sub> separation. *Microporous Mesoporous Mater* 312: 110761. <https://doi.org/10.1016/j.micromeso.2020.110761>
19. Bux H, Chmelik C, Krishna R, et al. (2011) Ethene/ethane separation by the MOF membrane ZIF-8: Molecular correlation of permeation, adsorption, diffusion. *J Membr Sci* 369: 284–289. <https://doi.org/10.1016/j.memsci.2010.12.001>
20. Shi Q, Song Z, Kang X, et al. (2012) Controlled synthesis of hierarchical zeolitic imidazolate framework-GIS (ZIF-GIS) architectures. *Cryst Eng Comm* 14: 8280–8285. <https://doi.org/10.1039/C2CE26170G>
21. Lai LS, Yeong YF, Ani NC, et al. (2014) Effect of synthesis parameters on the formation of Zeolitic Imidazolate Framework 8 (ZIF-8) nanoparticles for CO<sub>2</sub> adsorption. *Sep Sci Technol* 49: 520–528. <https://doi.org/10.1080/02726351.2014.920445>
22. Zeng X, Huang L, Wang C, et al. (2016) Sonocrystallization of ZIF-8 on electrostatic spinning TiO<sub>2</sub> nanofibers surface with enhanced photocatalysis property through synergistic effect. *ACS Appl Mater Interfaces* 8: 20274–20282. <https://doi.org/10.1021/acsami.6b05746>
23. Venna SR, Jasinski JB, Carreon MA (2010) Structural evolution of Zeolitic Imidazolate Framework-8. *J Am Chem Soc* 132: 7. <https://doi.org/10.1021/ja109268m>
24. Xiang L, Sheng L, Wang C, et al. (2017) Amino-functionalized ZIF-7 nanocrystals: Improved intrinsic separation ability and interfacial compatibility in mixed-matrix membranes for CO<sub>2</sub>/CH<sub>4</sub> separation. *Adv Mater* 29: 1–8. <https://doi.org/10.1002/adma.201606999>

25. Abdelhamid HN (2020) UiO-66 as a catalyst for hydrogen production via the hydrolysis of sodium borohydride. *Dalton Trans* 49: 10851. <https://doi.org/10.1039/D0DT01688H>
26. Abdelhaleem A, Abdelhamid HN, Ibrahim MG, et al. (2022) Photocatalytic degradation of paracetamol using photo-Fenton-like metal-organic framework-derived CuO@C under visible LED. *J Clean Prod* 379: 134571. <https://doi.org/10.1016/j.jclepro.2022.134571>
27. Madejski P, Chmiel K, Subramanian N, et al. (2022) Methods and techniques for CO<sub>2</sub> capture: Review of potential solutions and applications in modern energy technologies. *Energies* 15: 887. <https://doi.org/10.3390/en15030887>
28. Gładysz P, Stanek W, Czarnowska L, et al. (2018) Thermo-ecological evaluation of an integrated MILD oxy-fuel combustion power plant with CO<sub>2</sub> capture, utilization, and storage—A case study in Poland. *Energy* 144: 379–392. <https://doi.org/10.1016/j.energy.2017.11.133>
29. Tramošljika B, Blecich P, Bonefačić I, et al. (2021) Advanced ultra-supercritical coal-fired power plant with post-combustion carbon capture: Analysis of electricity penalty and CO<sub>2</sub> emission reduction. *Sustainability* 13: 1–20. <https://doi.org/10.3390/su13020801>
30. Holz F, Scherwath T, Crespo del Granado P, et al. (2021) A 2050 perspective on the role for carbon capture and storage in the European power system and industry sector. *Energy Econ* 104: 105631. <https://doi.org/10.1016/j.eneco.2021.105631>
31. Prat D, Wells A, Hayler J, et al. (2015) CHEM21 selection guide of classical-and less classical-solvents. *Green Chem* 18: 288. <https://doi.org/10.1039/C5GC01008J>
32. Kato M, Essaki K, Nakagawa K, et al. (2005) CO<sub>2</sub> absorption properties of lithium ferrite for application as a high-temperature CO<sub>2</sub> absorbent. *J Ceram Soc Jpn* 113: 684–686. <https://doi.org/10.2109/jcersj.113.684>
33. Samanta A, Zhao A, Shimizu GKH, et al. (2012) Post-combustion CO<sub>2</sub> capture using solid sorbents: A review. *Ind Eng Chem Res* 51: 1438–1463. <https://doi.org/10.1021/ie200686q>
34. Omoregbe O, Mustapha AN, Steinberger-Wilckens R, et al. (2020) Carbon capture technologies for climate change mitigation: A bibliometric analysis of the scientific discourse during 1998–2018. *Energy Rep* 6: 1200–1212. <https://doi.org/10.1016/j.egy.2020.05.003>
35. Yamauchi K, Murayama N, Shibata J (2007) Absorption and release of carbon dioxide with various metal oxides and hydroxides. *Mater Trans* 48: 2739–2742. <https://doi.org/10.2320/matertrans.M-MRA2007877>
36. Spataru CI, Ianchis R, Petcu C, et al. (2016) Synthesis of non-toxic silica particles stabilized by molecular complex oleic-acid/sodium oleate. *Int J Mol Sci* 17: 4–8. <https://doi.org/10.3390/ijms17111936>
37. Pimenidou P, Dupont V (2015) Dolomite study for in situ CO<sub>2</sub> capture for chemical looping reforming. *Int J Ambient Energy* 36: 170–182. <https://doi.org/10.1080/01430750.2013.841590>
38. Bhowan AS, Freeman BC (2011) Analysis and status of post-combustion carbon dioxide capture technologies. *Environ Sci Technol* 45: 23. <https://doi.org/10.1021/es104291d>
39. Feron PHM, Hendriks CA (2005) CO<sub>2</sub> capture process principles and costs. *Oil Gas Sci Technol* 60: 451–459. <https://doi.org/10.2516/ogst:2005027>
40. Yampolskii Y, Topchiev AV (2012) Polymeric gas separation membranes. *Russ Chem Rev* 81: 483–500. <https://doi.org/10.1021/ma300213b>
41. Siqueira RM, Freitas GR, Peixoto HR, et al. (2017) Carbon dioxide capture by pressure swing adsorption. *Energy Procedia* 114: 2182–2192. <https://doi.org/10.1016/j.egypro.2017.03.1355>

42. Yang MW, Chen NC, Huang CH, et al. (2014) Temperature swing adsorption process for CO<sub>2</sub> capture using polyaniline solid sorbent. *Energy Procedia* 63: 2351–2358. <https://doi.org/10.1016/j.egypro.2014.11.256>
43. Saenz Cavazos PA, Hunter-Sellars E, Iacomini P, et al. (2023) Evaluating solid sorbents for CO<sub>2</sub> capture: Linking material properties and process efficiency via adsorption performance. *Front Energy Res* 11: 1–22. <https://doi.org/10.3389/fenrg.2023.1167043>
44. Tsai CW, Langner EHG, Harris RA (2019) Computational study of ZIF-8 analogues with electron donating and withdrawing groups for CO<sub>2</sub> adsorption. *Microporous Mesoporous Mater* 288: 109613. <https://doi.org/10.1016/j.micromeso.2019.109613>
45. Junaidi MUM, Khoo CP, Leo CP, et al. (2014) The effects of solvents on the modification of SAPO-34 zeolite using 3-aminopropyl trimethoxy silane for the preparation of asymmetric polysulfone mixed matrix membrane in the application of CO<sub>2</sub> separation. *Microporous Mesoporous Mater* 192: 52–59. <https://doi.org/10.1016/j.micromeso.2013.10.006>
46. Song C, Liu Q, Deng S, et al. (2019) Cryogenic-based CO<sub>2</sub> capture technologies: State-of-the-art developments and current challenges. *Renew Sustain Energy Rev* 101: 265–278. <https://doi.org/10.1016/j.rser.2018.11.018>
47. Ahmed R, Liu G, Yousaf B, et al. (2020) Recent advances in carbon-based renewable adsorbent for selective carbon dioxide capture and separation—A review. *J Clean Prod* 242: 118409. <https://doi.org/10.1016/j.jclepro.2019.118409>
48. Zulkurnai NZ, Mohammad Ali UF, Ibrahim N, et al. (2017) Carbon dioxide (CO<sub>2</sub>) adsorption by activated carbon functionalized with deep eutectic solvent (DES). *IOP Conf Ser Mater Sci Eng* 206: 012030. <https://dx.doi.org/10.1088/1757-899X/206/1/012001>
49. Ngoy JM, Wagner N, Riboldi L, et al. (2014) A CO<sub>2</sub> capture technology using multi-walled carbon nanotubes with polyaspartamide surfactant. *Energy Procedia* 63: 2230–2248. <https://doi.org/10.1016/j.egypro.2014.11.242>
50. Singh S, Varghese AM, Reinalda D, et al. (2021) Graphene-based membranes for carbon dioxide separation. *J CO<sub>2</sub> Util* 49: 101544. <https://doi.org/10.1016/j.jcou.2021.101544>
51. Agrafioti E, Bouras G, Kalderis D, et al. (2013) Biochar production by sewage sludge pyrolysis. *J Anal Appl Pyrolysis* 101: 72–78. <https://doi.org/10.1016/j.jaap.2013.02.010>
52. Liu Y, Ren Y, Ma H, et al. (2022) Advanced organic molecular sieve membranes for carbon capture: Current status, challenges and prospects. *Adv Membr* 2: 100028. <https://doi.org/10.1016/j.advmem.2022.100028>
53. Yin M, Zhang L, Wei X, et al. (2022) Detection of antibiotics by electrochemical sensors based on metal-organic frameworks and their derived materials. *Microchem J* 183: 107946. <https://doi.org/10.1016/j.microc.2022.107946>
54. Rui Z, James JB, Lin YS (2018) Highly CO<sub>2</sub> perm-selective metal-organic framework membranes through CO<sub>2</sub> annealing post-treatment. *J Membr Sci* 555: 97–104. <https://doi.org/10.1016/j.memsci.2018.03.036>
55. Lee YR, Kim J, Ahn WS (2013) Synthesis of metal-organic frameworks: A mini review. *Korean J Chem Eng* 30: 1667–1680. <https://doi.org/10.1007/s11814-013-0140-6>
56. Demir H, Aksu GO, Gulbalkan HC, et al. (2022) MOF membranes for CO<sub>2</sub> capture: Past, present and future. *Carbon Capture Sci Technol* 2: 100026. <https://doi.org/10.1016/j.ccst.2021.100026>

57. Schaate A, Roy P, Godt A, et al. (2011) Modulated synthesis of Zr-based metal-organic frameworks: From nano to single crystals. *Chem Eur J* 17: 6643–6651. <https://doi.org/10.1002/chem.201003211>
58. Bux H, Feldhoff A, Cravillon J, et al. (2011) Oriented zeolitic imidazolate framework-8 membrane with sharp H<sub>2</sub>/C<sub>3</sub>H<sub>8</sub> molecular sieve separation. *Chem Mater* 23: 2262–2269. <https://doi.org/10.1021/cm200555s>
59. Chen Y, Tang S (2019) Solvothermal synthesis of porous hydrangea-like zeolitic imidazolate framework-8 (ZIF-8) crystals. *J Solid State Chem* 276: 68–74. <https://doi.org/10.1016/j.jssc.2019.04.034>
60. Ejeromedoghene O, Oderinde O, Okoye CO, et al. (2022) Microporous metal-organic frameworks based on deep eutectic solvents for adsorption of toxic gases and volatile organic compounds: A review. *Chem Eng J Adv* 12: 100361. <https://doi.org/10.1016/j.cej.2022.100361>
61. Park JH, Park SH, Jung SH (2009) Microwave-syntheses of zeolitic imidazolate framework material, ZIF-8. *J Korean Chem Soc* 53: 553–559. <https://doi.org/10.5012/jkcs.2009.53.5.553>
62. Cravillon J, Münzer S, Lohmeier SJ, et al. (2009) Rapid room-temperature synthesis and characterization of nanocrystals of a prototypical zeolitic imidazolate framework. *Chem Mater* 21: 1410–1412. <https://doi.org/10.1021/cm900166h>
63. Mullin JW (2001) Crystallization: Chapter 5—Nucleation, In: Mullin JW, *Crystallization*, Oxford: Butterworth-Heinemann, 181–215. <https://doi.org/10.1016/B978-075064833-2/50007-3>
64. Bazzi L, Ayouch I, Tachallait H, et al. (2022) Ultrasound and microwave assisted-synthesis of ZIF-8 from zinc oxide for the adsorption of phosphate. *Results Eng* 13: 100378. <https://doi.org/10.1016/j.rineng.2022.100378>
65. Beldon PJ, Fábíán L, Stein RS, et al. (2010) Rapid room-temperature synthesis of zeolitic imidazolate frameworks by using mechanochemistry. *Angew Chem Int Ed* 49: 9640–9643. <https://doi.org/10.1002/anie.201005547>
66. Bang JH, Suslick KS (2010) Applications of ultrasound to the synthesis of nanostructured materials. *Adv Mater* 22: 1039–1059. <https://doi.org/10.1002/adma.200904093>
67. Cho HY, Kim J, Kim SN, et al. (2012) High yield 1-L scale synthesis of ZIF-8 via a sonochemical route. *Microporous Mesoporous Mater* 156: 171–177. <https://doi.org/10.1016/j.micromeso.2012.11.012>
68. Chalati T, Horcajada P, Gref R, et al. (2010) Optimisation of the synthesis of MOF nanoparticles made of flexible porous iron fumarate MIL-88A. *J Mater Chem* 20: 7676–7681. <https://doi.org/10.1039/C0JM03563G>
69. Pichon A, Lazuen-Garay A, James SL (2006) Solvent-free synthesis of a microporous metal-organic framework. *CrystEngComm* 8: 211–214. <https://doi.org/10.1039/B513750K>
70. Carson CG, Brown AJ, Sholl DS, et al. (2022) Sonochemical synthesis and characterization of submicrometer crystals of the metal-organic framework Cu[(hfipbb)(H<sub>2</sub>hfipbb)<sub>0.5</sub>]. *J Mater Chem* 19: 18. <https://doi.org/10.1021/cg200728b>
71. Seyedin S, Zhang J, Usman KAS, et al. (2019) Facile solution processing of stable MXene dispersions towards conductive composite fibers. *Glob Chall* 3: 1900037. <https://doi.org/10.1002/gch2.201900037>
72. Venna SR, Carreon MA (2010) Highly permeable zeolite imidazolate framework-8 membranes for CO<sub>2</sub>/CH<sub>4</sub> separation. *J Am Chem Soc* 132: 76–78. <https://doi.org/10.1021/ja909263x>



73. Son WJ, Choi JS, Ahn WS (2008) Adsorptive removal of carbon dioxide using polyethyleneimine-loaded mesoporous silica materials. *Microporous Mesoporous Mater* 113: 31–40. <https://doi.org/10.1016/j.micromeso.2007.10.049>
74. Klimakow M, Klobes P, Thünemann AF, et al. (2010) Mechanochemical synthesis of metal-organic frameworks: a fast and facile approach toward quantitative yields and high specific surface areas. *Chem Mater* 22: 5216–5221. <https://doi.org/10.1021/cm1012119>
75. Yue Y, Qiao ZA, Li X, et al. (2013) Nanostructured zeolitic imidazolate frameworks derived from nanosized zinc oxide precursors. *Cryst Growth Des* 13: 1002–1005. <https://doi.org/10.1021/cg4002362>
76. Usman KAS, Maina JW, Seyedin S, et al. (2020) Downsizing metal–organic frameworks by bottom-up and top-down methods. *NPG Asia Mater* 12: 58. <https://doi.org/10.1038/s41427-020-00240-5>
77. Ogura M, Nakata SI, Kikuchi E, et al. (2001) Effect of  $\text{NH}_4^+$  exchange on hydrophobicity and catalytic properties of Al-free Ti–Si–beta zeolite. *J Catal* 199: 41–47. <https://doi.org/10.1006/jcat.2000.3156>
78. Gökpınar S, Diment T, Janiak C (2017) Environmentally benign dry-gel conversions of Zr-based UiO metal–organic frameworks with high yield and the possibility of solvent re-use. *Dalton Trans* 46: 9895. <https://doi.org/10.1039/C7DT01717K>
79. Awadallah-F A, Hillman F, Al-Muhtaseb SA, et al. (2019) Nano-gate opening pressures for the adsorption of isobutane, n-butane, propane, and propylene gases on bimetallic Co–Zn based zeolitic imidazolate frameworks. *Microporous Mesoporous Mater* 48: 4685. <https://doi.org/10.1039/C9DT00222G>
80. Tannert N, Gökpınar S, Hastürk E, et al. (2018) Microwave-assisted dry-gel conversion—A new sustainable route for the rapid synthesis of metal-organic frameworks with solvent re-use. *Dalton Trans* 47: 9850–9860. <https://doi.org/10.1039/C8DT02029A>
81. Ahmed I, Jeon J, Khan NA, et al. (2012) Synthesis of a metal–organic framework, iron-benzenetricarboxylate, from dry gels in the absence of acid and salt. *Cryst Growth Des* 12: 5878–5881. <https://doi.org/10.1021/cg3014317>
82. Jahn A, Reiner JE, Vreeland WN, et al. (2008) Preparation of nanoparticles by continuous-flow microfluidics. *J Nanopart Res* 10: 925–934. <https://doi.org/10.1007/s11051-007-9340-5>
83. Lee YR, Jang MS, Cho HY, et al. (2015) ZIF-8: A comparison of synthesis methods. *Chem Eng J* 271: 276–280. <https://doi.org/10.1016/j.cej.2015.02.094>
84. Kolmykov O, Commenge JM, Alem H, et al. (2017) Microfluidic reactors for the size-controlled synthesis of ZIF-8 crystals in aqueous phase. *Mater Des* 122: 31–41. <https://doi.org/10.1016/j.matdes.2017.03.002>
85. Schejn A, Frégnaux M, Commenge JM, et al. (2014) Size-controlled synthesis of ZnO quantum dots in microreactors. *Nanotechnology* 25. <https://iopscience.iop.org/article/10.1088/0957-4484/25/14/145606/data>
86. Gross AF, Sherman E, Vajo JJ (2012) Aqueous room temperature synthesis of cobalt and zinc sodalite zeolitic imidazolate frameworks. *Dalton Trans* 41: 5458–5460. <https://doi.org/10.1039/C2DT30174A>
87. Faustini M, Kim J, Jeong GY, et al. (2013) Microfluidic approach toward continuous and ultrafast synthesis of metal–organic framework crystals and hetero structures in confined microdroplets. *J Am Chem Soc* 135: 14619–14626. <https://doi.org/10.1021/ja4039642>

88. Yamamoto D, Maki T, Watanabe S, et al. (2013) Synthesis and adsorption properties of ZIF-8 nanoparticles using a micromixer. *Chem Eng J* 227: 145–150. <https://doi.org/10.1016/j.cej.2012.08.065>
89. Butova VV, Soldatov MA, Guda AA, et al. (2016) Metal-organic frameworks: structure, properties, methods of synthesis and characterization. *Russ Chem Rev* 85: 280–307. <https://iopscience.iop.org/article/10.1070/RCR4554>
90. Butova VV, Budnyk AP, Bulanov EA, et al. (2017) Hydrothermal synthesis of high surface area ZIF-8 with minimal use of TEA. *Solid State Sci* 69: 13–21. <https://doi.org/10.1016/j.solidstatesciences.2017.05.002>
91. Riley BJ, Vienna JD, Strachan DM, et al. (2016) Materials and processes for the effective capture and immobilization of radioiodine: A review. *J Nucl Mater* 470: 307–326. <https://doi.org/10.1016/j.jnucmat.2015.11.038>
92. Saini K, Yadav S, Jain M, et al. (2021) Recent advances and challenges in selective environmental applications of metal-organic frameworks. *ACS Symp Ser* 1394: 223–245. <http://dx.doi.org/10.1021/bk-2021-1394.ch009>
93. Lestari G (2012) Hydrothermal synthesis of zeolitic imidazolate frameworks-8 (ZIF-8) crystals with controllable size and morphology. MS Thesis, King Abdullah University of Science and Technology. <https://doi.org/10.25781/KAUST-461G0>
94. Pan Y, Liu Y, Zeng G, et al. (2011) Rapid synthesis of zeolitic imidazolate framework-8 (ZIF-8) nanocrystals in an aqueous system. *Chem Commun* 47: 2071–2073. <https://doi.org/10.1039/C0CC05002D>
95. Huang XC, Lin YY, Zhang JP, et al. (2006) Ligand-directed strategy for zeolite-type metal-organic frameworks: Zinc(ii) imidazoles with unusual zeolitic topologies. *Angew Chem Int Ed* 45: 1557–1559. <https://doi.org/10.1002/anie.200503778>
96. Chiang YC, Chin WT, Huang CC (2021) The application of hollow carbon nanofibers prepared by electrospinning to carbon dioxide capture. *J Mater Sci* 56: 2490–2502. <https://doi.org/10.3390/polym13193275>
97. Malekmohammadi M, Fatemi S, Razavian M, et al. (2019) A comparative study on ZIF-8 synthesis in aqueous and methanolic solutions: Effect of temperature and ligand content. *Solid State Sci* 91: 108–112. <https://doi.org/10.1016/j.solidstatesciences.2019.03.022>
98. Xian S, Xu F, Ma C, et al. (2015) Vapor-enhanced CO<sub>2</sub> adsorption mechanism of composite PEI@ZIF-8 modified by polyethyleneimine for CO<sub>2</sub>/N<sub>2</sub> separation. *Chem Eng J* 280: 363–369. <https://doi.org/10.1016/j.cej.2015.06.042>
99. Hao F, Yan XP (2022) Nano-sized zeolite-like metal-organic frameworks induced hematological effects on red blood cell. *J Hazard Mater* 424: 127353. <https://doi.org/10.1016/j.jhazmat.2021.127353>
100. Zheng W, Ding R, Yang K, et al. (2019) ZIF-8 nanoparticles with tunable size for enhanced CO<sub>2</sub> capture of Pebax based MMMs. *Sep Purif Technol* 214: 111–119. <https://doi.org/10.1016/j.seppur.2018.04.010>
101. Jiang HL, Liu B, Akita T, et al. (2009) Au@ZIF-8: CO oxidation over gold nanoparticles deposited to metal-organic framework. *J Am Chem Soc* 131: 11302–11303. <https://doi.org/10.1021/ja9047653>

102. Kong X, Yu Y, Ma S, et al. (2018) Adsorption mechanism of H<sub>2</sub>O molecule on the Li<sub>4</sub>SiO<sub>4</sub> (010) surface from first principles. *Chem Phys Lett* 691: 1–7. <https://doi.org/10.1016/j.cplett.2017.10.054>
103. Chen B, Yang Z, Zhu Y, et al. (2014) Zeolitic imidazolate framework materials: recent progress in synthesis and applications *J Mater Chem A* 2: 16811–16831. <https://doi.org/10.1039/C4TA02984D>
104. Chiang YC, Chin WT (2022) Preparation of zeolitic imidazolate framework-8-based nanofiber composites for carbon dioxide adsorption. *Nanomaterials* 12: 1492. <https://doi.org/10.3390/nano12091492>
105. Aulia W, Ahnaf A, Irianto MY, et al. (2020) Synthesis and characterization of zeolitic imidazolate framework-8 (ZIF-8)/Al<sub>2</sub>O<sub>3</sub> composite. *IPTEK* 31: 18–24. <https://doi.org/10.12962/j20882033.v31i1.5511>
106. Su Z, Zhang M, Lu Z, et al. (2018) Functionalization of cellulose fiber by in situ growth of zeolitic imidazolate framework-8 (ZIF-8) nanocrystals for preparing a cellulose-based air filter with gas adsorption ability. *Cellulose* 25: 1997–2008. <https://doi.org/10.1007/s10570-018-1696-4>
107. Payra S, Challagulla S, Indukuru RR, et al (2018) The structural and surface modification of zeolitic imidazolate frameworks towards reduction of encapsulated CO<sub>2</sub>. *New J Chem* 42: 19205–19213. <https://doi.org/10.1039/C8NJ04247K>
108. Chen R, Yao J, Gu Q, et al. (2013) A two-dimensional zeolitic imidazolate framework with a cushion-shaped cavity for CO<sub>2</sub> adsorption. *Chem Commun* 49: 9500. <https://doi.org/10.1039/C3CC44342F>
109. Awadallah-F A, Hillman F, Al-Muhtaseb SA, et al. (2019) On the nanogate-opening pressures of copper-doped zeolitic imidazolate framework ZIF-8 for the adsorption of propane, propylene, isobutane, and n-butane. *J Mater Sci* 54: 5513–5527. <https://doi.org/10.1007/s10853-018-03249-y>
110. Cho HY, Kim J, Kim SN, et al. (2013) High yield 1-L scale synthesis of ZIF-8 via a sonochemical route. *Micropor Mesopor Mat* 169: 180–184. <https://doi.org/10.1016/j.micromeso.2012.11.012>
111. Fu F, Zheng B, Xie LH, et al. (2018) Size-controllable synthesis of zeolitic imidazolate framework/carbon nanotube composites. *Crystals* 8: 367. <https://doi.org/10.3390/cryst8100367>
112. Du PD, Hieu NT, Thien TV (2021) Ultrasound-assisted rapid ZIF-8 synthesis, porous ZnO preparation by heating ZIF-8, and their photocatalytic activity. *J Nanomater* 2021: 9988998. <https://doi.org/10.1155/2021/9988998>
113. Modi A, Jiang Z, Kasher R (2022) Hydrostable ZIF-8 layer on polyacrylonitrile membrane for efficient treatment of oilfield produced water. *Chem Eng J* 434: 133513. <https://doi.org/10.1016/j.cej.2021.133513>
114. Mphuthi LE, Erasmus E, Langner EHG (2021) Metal exchange of ZIF-8 and ZIF-67 nanoparticles with Fe(II) for enhanced photocatalytic performance. *ACS Omega* 6: 31632–31645. <https://doi.org/10.1021/acsomega.1c04142>
115. Wu T, Dong J, De France K, et al. (2020) Porous carbon frameworks with high CO<sub>2</sub> capture capacity derived from hierarchical polyimide/zeolitic imidazolate frameworks composite aerogels. *Chem Eng J* 395: 124927. <https://doi.org/10.1016/j.cej.2020.124927>
116. Aceituno Melgar VM, Ahn H, Kim J, et al. (2015) Zeolitic imidazolate framework membranes for gas separation: A review of synthesis methods and gas separation performance. *J Ind Eng Chem* 28: 1–15. <https://doi.org/10.1016/j.jiec.2015.03.006>

117. Drobek M, Bechelany M, Vallicari C, et al. (2015) An innovative approach for the preparation of confined ZIF-8 membranes by conversion of ZnO ALD layers. *J Membr Sci* 475: 39–46. <https://doi.org/10.1016/j.memsci.2014.10.011>
118. Kenyotha K, Chanapatttharapol KC, McCloskey S (2020) Water based synthesis of ZIF-8 assisted by hydrogen bond acceptors and enhancement of CO<sub>2</sub> uptake by solvent assisted ligand exchange. *Crystals* 10: 599. <https://doi.org/10.3390/cryst10070599>
119. Ding B, Wang X, Xu Y, et al. (2018) Hydrothermal preparation of hierarchical ZIF-L nanostructures for enhanced CO<sub>2</sub> capture. *J Colloid Interface Sci* 519: 38–43. <https://doi.org/10.1016/j.jcis.2018.02.047>
120. Chen Y, Wang B, Zhao L, et al. (2015) New Pebax®/zeolite Y composite membranes for CO<sub>2</sub> capture from flue gas. *J Membr Sci* 495: 415–423. <https://doi.org/10.1016/j.memsci.2015.08.045>
121. McEwen J, Hayman JD, Ozgur Yazaydin A, et al. (2013) A comparative study of CO<sub>2</sub>, CH<sub>4</sub> and N<sub>2</sub> adsorption in ZIF-8, Zeolite-13X and BPL activated carbon. *Chem Phys* 412: 72–76. <https://doi.org/10.1016/j.chemphys.2012.12.012>
122. Papchenko K, Risaliti G, Ferroni M, et al. (2021) An analysis of the effect of ZIF-8 addition on the separation properties of polysulfone at various temperatures. *Membranes* 11: 427. <https://doi.org/10.3390/membranes11060427>
123. Ma H, Wang Z, Zhang XF, et al. (2021) In situ growth of amino-functionalized ZIF-8 on bacterial cellulose foams for enhanced CO<sub>2</sub> adsorption. *Carbohydr Polym* 270: 118376. <https://doi.org/10.1016/j.carbpol.2021.118376>
124. Korelskiy D, Ye P, Fouladvand S, et al. (2015) Efficient ceramic zeolite membranes for CO<sub>2</sub>/H<sub>2</sub> separation. *J Mater Chem A* 3: 12500–12506. <https://doi.org/10.1039/C5TA02152A>
125. Ban Y, Li Y, Peng Y, et al. (2014) Metal-substituted zeolitic imidazolate framework ZIF-108: Gas-sorption and membrane-separation properties. *Chem Eur J* 20: 11402–11409. <https://doi.org/10.1002/chem.201402287>
126. Al Abdulla S, Sabouni R, Ghommam M, et al. (2023) Synthesis and performance analysis of zeolitic imidazolate frameworks for CO<sub>2</sub> sensing applications. *Heliyon* 9: e21349. <https://doi.org/10.1016/j.heliyon.2023.e21349>
127. Wang B, Côté AP, Furukawa H, et al. (2008) Colossal cages in zeolitic imidazolate frameworks as selective carbon dioxide reservoirs. *Nature* 453: 207–211. <https://doi.org/10.1038/nature06900>
128. Banerjee R, Phan A, Wang B, et al. (2008) High-throughput synthesis of zeolitic imidazolate frameworks and application to CO<sub>2</sub> capture. *Science* 319: 939–943. <https://doi.org/10.1126/science.1152516>
129. Chen C, Kim J, Yang DA, et al. (2011) Carbon dioxide adsorption over zeolite-like metal-organic frameworks (ZMOFs) having a sod topology: Structure and ion-exchange effect. *Chem Eng J* 168: 1134–1139. <https://doi.org/10.1016/j.cej.2011.01.096>
130. Shieh FK, Wang SC, Leo SY, et al. (2013) Water-based synthesis of zeolitic imidazolate framework-90 (ZIF-90) with a controllable particle size. *Chem Eng J* 19: 11139–11142. <https://doi.org/10.1002/chem.201301560>
131. Tien-Binh N, Rodrigue D, Kaliaguine S (2018) In-situ cross interface linking of PIM-1 polymer and UiO-66-NH<sub>2</sub> for outstanding gas separation and physical aging control. *J Membr Sci* 548: 429–438. <https://doi.org/10.1016/j.memsci.2017.11.054>

132. Vedrtnam A, Kalauni K, Dubey S, et al. (2020) A comprehensive study on structure, properties, synthesis, and characterization of ferrites. *AIMS Mater Sci* 7: 800–835. <https://doi.org/10.3934/matersci.2020.6.800>
133. Vendite AC, Soares TA, Coutinho K (2022) The effect of surface composition on the selective capture of atmospheric CO<sub>2</sub> by ZIF nanoparticles: The case of ZIF-8. *J Chem Inf Model* 62: 6530–6543. <https://doi.org/10.1021/acs.jcim.2c00579>
134. Railey P, Song Y, Liu T, et al. (2017) Metal-organic frameworks with immobilized nanoparticles: Synthesis and applications in photocatalytic hydrogen generation and energy storage. *Mater Res Bull* 96: 385–394. <https://doi.org/10.1016/j.materresbull.2017.04.020>
135. Keskin S, van Heest TM, Sholl DS (2010) Can metal-organic framework materials play a useful role in large-scale carbon dioxide separations? *ChemSusChem* 3: 879–891. <https://doi.org/10.1002/cssc.201000114>
136. Abraha YW, Tsai CW, Niemantsverdriet JWH, et al. (2021) Optimized CO<sub>2</sub> capture of the zeolitic imidazolate framework ZIF-8 modified by solvent-assisted ligand exchange. *ACS Omega* 6: 21850–21860. <https://doi.org/10.1021/acsomega.1c01130>
137. Karagiari O, Lalonde MB, Bury W, et al. (2012) Opening ZIF-8: A catalytically active zeolitic imidazolate framework of sodalite topology with unsubstituted linkers. *J Am Chem Soc* 134: 18790–18796. <https://doi.org/10.1021/ja308786r>
138. Jayachandrababu KC, Sholl DS, Nair S (2017) Structural and mechanistic differences in mixed-linker zeolitic imidazolate framework synthesis by solvent-assisted linker exchange and de novo routes. *J Am Chem Soc* 139: 5906–5915. <https://doi.org/10.1021/jacs.7b01660>
139. Wang P, Liu J, Liu C, et al. (2016) Electrochemical synthesis and catalytic properties of encapsulated metal clusters within zeolitic imidazolate frameworks. *Chem Eur J* 22: 16613–16620. <https://doi.org/10.1002/chem.201602924>
140. Phan A, Doonan CJ, Uribe-Romo FJ, et al. (2010) Synthesis, structure, and carbon dioxide capture properties of zeolitic imidazolate frameworks. *Acc Chem Res* 43: 58–67. <https://doi.org/10.1021/ar900116g>
141. Marti AM, Wickramanayake W, Dahe G, et al. (2017) Continuous flow processing of ZIF-8 membranes on polymeric porous hollow fiber supports for CO<sub>2</sub> capture. *ACS Appl Mater Interfaces* 9: 5678–5682. <https://doi.org/10.1021/acsami.6b15619>
142. Chen B, Bai F, Zhu Y, et al. (2014) A cost-effective method for the synthesis of zeolitic imidazolate framework-8 materials from stoichiometric precursors via aqueous ammonia modulation at room temperature. *Microporous Mesoporous Mater* 193: 7–14. <https://doi.org/10.1016/j.micromeso.2014.03.006>
143. Lai LS, Yeong YF, Lau KK, et al. (2016) Effect of synthesis parameters on the formation of ZIF-8 under microwave-assisted solvothermal conditions. *Procedia Eng* 148: 35–42. <https://doi.org/10.1016/j.proeng.2016.06.481>
144. Jiang S, Liu J, Guan J, et al. (2023) Enhancing CO<sub>2</sub> adsorption capacity of ZIF-8 by synergetic effect of high pressure and temperature. *Sci Rep* 13: 1–10. <https://doi.org/10.1038/s41598-023-44960-4>
145. Pouramini Z, Mousavi SM, Babapoor A, et al. (2023) Effect of metal atom in zeolitic imidazolate frameworks. *Catalysts* 13: 155. <https://doi.org/10.3390/catal13010155>

146. Latrach Z, Moumen E, Kounbach S, et al. (2022) Mixed-ligand strategy for the creation of hierarchical porous ZIF-8 for enhanced adsorption of copper ions. *ACS Omega* 7: 12345–12354. <https://doi.org/10.1021/acsomega.2c00980>
147. Hu J, Liu Y, Liu J, et al. (2017) Effects of water vapor and trace gas impurities in flue gas on CO<sub>2</sub> capture in zeolitic imidazolate frameworks: The significant role of functional groups. *Fuel* 200: 244–251. <https://doi.org/10.1016/j.fuel.2017.03.079>
148. Liu Y, Kasik A, Linneen N, et al. (2014) Adsorption and diffusion of carbon dioxide on ZIF-68. *Chem Eng Sci* 118: 32–40. <https://doi.org/10.1016/j.ces.2014.07.030>
149. Liu Y, Liu J, Chang M, et al. (2012) Theoretical studies of CO<sub>2</sub> adsorption mechanism on linkers of metal–organic frameworks. *Fuel* 95: 521–527. <https://doi.org/10.1016/j.fuel.2011.09.057>
150. Gu C, Liu Y, Wang W, et al. (2021) Effects of functional groups for CO<sub>2</sub> capture using metal-organic frameworks. *Front Chem Sci Eng* 15: 437–449 <https://doi.org/10.1007/s11705-020-1961-6>
151. Yang F, Ge T, Zhu X, et al. (2022) Study on CO<sub>2</sub> capture in humid flue gas using amine-modified ZIF-8. *Sep Purif Technol* 287: 120535. <https://doi.org/10.1016/j.seppur.2022.120535>
152. Ji Y, Liu X, Li H, et al. (2023) Hydrophobic ZIF-8 covered active carbon for CO<sub>2</sub> capture from humid gas. *J Ind Eng Chem* 121: 331–337. <https://doi.org/10.1016/j.jiec.2023.01.036>
153. Xu H, Cheng W, Jin X, et al. (2013) Effect of the particle size of quartz powder on the synthesis and CO<sub>2</sub> absorption properties of Li<sub>4</sub>SiO<sub>4</sub> at high temperature. *Ind Eng Chem Res* 52: 1886–1891. <https://doi.org/10.1021/ie301178p>
154. Li Z, Cao Z, Grande C, et al. (2021) A phase conversion method to anchor ZIF-8 onto a PAN nanofiber surface for CO<sub>2</sub> capture. *RSC Adv* 12: 664–670. <https://doi.org/10.1039/D1RA06480K>
155. Åhlén M, Jaworski A, Strømme M, et al. (2021) Selective adsorption of CO<sub>2</sub> and SF<sub>6</sub> on mixed-linker ZIF-7–8s: The effect of linker substitution on uptake capacity and kinetics. *Chem Eng J* 422: 130117. <https://doi.org/10.1016/j.cej.2021.130117>
156. Asadi E, Ghadimi A, Hosseini SS, et al. (2022) Surfactant-mediated and wet-impregnation approaches for modification of ZIF-8 nanocrystals: Mixed matrix membranes for CO<sub>2</sub>/CH<sub>4</sub> separation. *Microporous Mesoporous Mater* 329: 111539. <https://doi.org/10.1016/j.micromeso.2021.111539>
157. Zhang H, Duan C, Li F, et al. (2018) Green and rapid synthesis of hierarchical porous zeolitic imidazolate frameworks for enhanced CO<sub>2</sub> capture. *Inorg Chim Acta* 482: 358–363. <https://doi.org/10.1016/j.ica.2018.06.034>
158. Martinez Joaristi A, Juan-Alcañiz J, Serra-Crespo P, et al. (2012) Electrochemical synthesis of some archetypical Zn<sup>2+</sup>, Cu<sup>2+</sup>, and Al<sup>3+</sup> metal-organic frameworks. *Cryst Growth Des* 12: 3489–3498. <https://doi.org/10.1021/cg300552w>
159. Zhang X, Yuan N, Chen T, et al. (2022) Fabrication of hydrangea-shaped Bi<sub>2</sub>WO<sub>6</sub>/ZIF-8 visible-light responsive photocatalysts for degradation of methylene blue. *Chemosphere* 307: 135678. <https://doi.org/10.1016/j.chemosphere.2022.135949>
160. Liu X, Gao F, Xu J, et al. (2016) Zeolite@mesoporous silica-supported-amine hybrids for the capture of CO<sub>2</sub> in the presence of water. *Microporous Mesoporous Mater* 222: 113–119. <https://doi.org/10.1016/j.micromeso.2015.10.006>
161. Sebastián V, Kumakiri I, Bredesen R, et al. (2007) Zeolite membrane for CO<sub>2</sub> removal: Operating at high pressure. *J Membr Sci* 292: 92–97. <https://doi.org/10.1016/j.memsci.2007.01.017>

162. Erkartal M, Incekara K, Sen U (2022) Synthesis of benzotriazole functionalized ZIF-8 by postsynthetic modification for enhanced CH<sub>4</sub> and CO<sub>2</sub> uptakes. *Inorg Chem Commun* 142: 109696. <https://doi.org/10.1016/j.inoche.2022.109696>
163. Bolotov VA, Kovalenko KA, Samsonenko DG, et al. (2018) Enhancement of CO<sub>2</sub> uptake and selectivity in a metal–organic framework by the incorporation of thiophene functionality. *Inorg Chem* 57: 5074–5082. <https://doi.org/10.1021/acs.inorgchem.8b00138>
164. Shi GM, Yang T, Chung TS (2012) Polybenzimidazole (PBI)/zeolitic imidazolate frameworks (ZIF-8) mixed matrix membranes for pervaporation dehydration of alcohols. *J Membr Sci* 415–416: 577–586. <https://doi.org/10.1016/j.memsci.2012.05.052>
165. Yang T, Chung TS (2013) High performance ZIF-8/PBI nano-composite membranes for high temperature hydrogen separation consisting of carbon monoxide and water vapor. *Int J Hydrogen Energy* 38: 229–239. <https://doi.org/10.1016/j.ijhydene.2012.10.045>
166. Abdelhamid HN, Mathew AP (2021) In-situ growth of zeolitic imidazolate frameworks into a cellulosic filter paper for the reduction of 4-nitrophenol. *Carbohydr Polym* 274: 118657. <https://doi.org/10.1016/j.carbpol.2021.118657>
167. Ding M, Flaig RW, Jiang HL, et al. (2019) Carbon capture and conversion using metal–organic frameworks and MOF-based materials. *Chem Soc Rev* 48: 2783–2828. <https://doi.org/10.1039/C8CS00829A>
168. Liu D, Ma X, Xi H, et al. (2014) Gas transport properties and propylene/propane separation characteristics of ZIF-8 membranes. *J Membr Sci* 451: 85–93. <https://doi.org/10.1016/j.memsci.2013.09.029>
169. Reza Abbasi A, Moshtkob A, Shahabadi N, et al. (2019) Synthesis of nano zinc-based metal–organic frameworks under ultrasound irradiation in comparison with solvent-assisted linker exchange: Increased storage of N<sub>2</sub> and CO<sub>2</sub>. *Ultrason Sonochem* 59: 104729. <https://doi.org/10.1016/j.ultsonch.2019.104729>
170. Hu Z, Zhang H, Zhang XF, et al. (2022) Polyethylenimine grafted ZIF-8@cellulose acetate membrane for enhanced gas separation. *J Membr Sci* 662: 120996. <https://doi.org/10.1016/j.memsci.2022.120996>



AIMS Press

© 2025 the Author(s), licensee AIMS Press. This is an open access article distributed under the terms of the Creative Commons Attribution License (<http://creativecommons.org/licenses/by/4.0>)